Engineering Design Earthquakes from Multimodal Hazard Disaggregation

Iunio Iervolino[1,*], Eugenio Chioccarelli[1] and Vincenzo Convertito[2].

[1]*Dipartimento di Ingegneria Strutturale Università degli Studi di Napoli Federico II, Naples, Italy.*

[2]*Istituto Nazionale di Geofisica e Vulcanologia, Osservatorio Vesuviano, Naples, Italy.*

Abstract

To define reference structural actions, engineers practicing earthquake resistant design are required by codes to account for ground motion likely to threaten the site of interest and also for pertinent seismic source features. In most of the cases, while the former issue is addressed assigning a mandatory design response spectrum, the latter is left unsolved. However, in the case that the design spectrum is derived from probabilistic seismic hazard analysis, disaggregation may be helpful, allowing to identify the earthquakes having the largest contribution to the hazard for the spectral ordinates of interest. Such information may also be useful to engineers in better defining the design scenario for the structure; e.g., in record selection for nonlinear seismic structural analysis. On the other hand, disaggregation results change with the spectral ordinate and return period, and more than a single event may dominate the hazard, especially if multiple sources affect the hazard at the site. This work discusses identification of engineering design earthquakes referring, as an example, to the Italian case. The considered hazard refers to exceedance of peak ground acceleration and 1s spectral acceleration with four return periods between 50 and 2475 years. It is discussed how, for most of the Italian sites, more than a design earthquake exists, because of the modelling of seismic sources. Furthermore, it is explained how and why these change with the limit state and the dynamic properties of the structure. Finally, it is illustrated how these concepts may be easily included in engineering practice complementing design hazard maps and effectively enhancing definition of design seismic actions with relatively small effort.

Keywords: Performance-Based Earthquake Engineering, Record Selection, Seismic Scenario, Seismic Actions, Design Spectrum.

1. Introduction

Earthquake resistant design in international seismic codes relies widely on a target spectrum to define seismic actions on structures. Being a synthetic representation of ground motion, the design

[*] Corresponding author: Iunio Iervolino, Dipartimento di Ingegneria Strutturale, Università degli Studi di Napoli Federico II, via Claudio 21, 80125, Naples, Italy. Tel: +390817683488; Fax: +390817685921; e-mail: iunio.iervolino@unina.it

spectrum should implicitly include information about the features of the seismogenetic sources determining the seismic hazard at the construction site. Nevertheless, prudently, the practitioner is often required to also account explicitly for them, for example, when dealing with ground motion record selection as input for nonlinear seismic structural analyses (e.g., [1] and [2]). For example, Eurocode 8 [3], or EC8 provides that: *In the range of periods between $0.2T_1$ and $2T_1$, where T_1 is the fundamental period of the structure in the direction where the accelerogram will be applied, no value of the mean 5% damping elastic spectrum, calculated from all time histories, should be less than 90% of the corresponding value of the 5% damping elastic response spectrum*. Moreover, accelerograms should be *adequately qualified with regard to the seismogenetic features of the sources* […].

In most of the cases, it is unlikely that the engineer has the information and/or is able to qualify the input ground motions with respect to the seismological features of the seismic sources[1]. However, if the design spectrum is related to probabilistic seismic hazard analysis (PSHA), it is possible to obtain *design earthquakes* (DEs) in terms of magnitude, location and other parameters such as faulting style, hanging/foot wall, etc.

In fact, PSHA allows one to compute the average return period of ground motions exceeding a given intensity measure (IM) threshold at the considered site [4]. On the other hand, if the return period of seismic action for design purposes is defined *a-priori*, and if the IM is the elastic spectral acceleration at different structural periods, it is possible to build the uniform hazard spectrum (UHS); i.e., the response spectrum with a constant exceedance probability for all ordinates; e.g., 10% in 50 years (or, equivalently, 475 yr return period) in the case of design for life-safety structural performance [5]. UHS is not the only possible PSHA-based design spectrum [6], but it is, to date, the basis for the definition of design seismic actions on structures in the most advanced seismic codes [7]. In fact, the Italian seismic code is based on the work of the *Instituto Nazionale di*

[1] EC8 actually requires information about seismic source also in choosing between two possible design spectrum shapes stating that: *If the earthquakes that contribute most to the seismic hazard defined for the site for the purpose of probabilistic hazard assessment have a surface-wave magnitude, Ms, not greater than 5.5, it is recommended that the Type 2 spectrum is adopted.*

Geofisica e Vulcanologia (INGV) which computed uniform hazard spectra (UHS) over a grid of more than 10000 points for 9 return periods (Tr) from 30yr to 2475yr, and 10 spectral ordinates, from 0.1s to 2.0s (http://esse1.mi.ingv.it/). As a consequence, at each site, Italian design spectra are a close approximation of the UHS.

If UHS is the design spectrum, *disaggregation* of seismic hazard [8] identifies the values of some earthquake characteristics providing the largest contributions to the hazard in terms of exceeding a specified spectral ordinate threshold. These events may be referred to as the earthquakes dominating the seismic hazard in a probabilistic sense, and may be used as DEs, as conceptually introduced by McGuire [4]. In a previous work (i.e., [9]) the authors elaborated on this topic referring to a case-study region in southern Italy. Herein, the issues raised about identification of DEs are investigated further and taken to a national level. This is relevant because modern codes increasingly rely on PSHA to define design spectra yet giving limited, if any, information about design scenarios. It may be useful, then, to develop tools, complementary to design spectra and hazard maps based on disaggregation, which allow the practitioner to identify the scenario seismic events of interest (e.g., maps of DEs), as also invoked by Bommer [10].

In the presented study DEs are identified disaggregating the probabilistic seismic hazard, computed for two spectral ordinates intended to represent the short and moderate period portions of the response spectrum, and four return periods. Disaggregation is expressed in terms magnitude (M), source to site distance (R) and ε (the number of standard deviations that the ground motion parameter is away from its median value estimated by the assumed attenuation relationship).

Along with mapping of design events, it is shown first that, for the most Italian sites, two DEs exist, a moderate-close one and a strong-distant one, and it is explained why this depends on the modeling of seismic sources considered in PSHA. Secondly, results of the study include discussion of how and why DEs change with the spectral ordinate (i.e., the dynamic characteristics of the considered structure), the return period of the seismic action and with relative distance to seismogenic zones. It is also demonstrated why, although it may sound counterintuitive [9], the

contribution of the moderate-close event increases with the return period with respect to the strong-distant earthquake. Finally, it is illustrated how maps of DEs may be easy yet useful complements to design acceleration maps, for both ordinary and advanced engineering practice.

2. Methodology

Given a seismic source model and a ground-motion prediction equation (GMPE), PSHA provides, for a selected site, the hazard curve representing the mean annual frequency of exceedance of a ground motion IM. Starting from PSHA results, disaggregation is a procedure which allows identification of the hazard contribution of each {M, R, ε} vector. The analytical result of disaggregation is the joint probability density function[2] (PDF) of {M, R, ε} conditional to the exceedance of an IM threshold (IM_0), Eq. (1).

$$f\left(m,r,\varepsilon \middle| IM > IM_0\right) = \frac{\sum_{i=1}^{n} \nu_i \cdot I\left[IM > IM_0 \middle| m,r,\varepsilon\right] \cdot f\left(m,r,\varepsilon\right)}{\lambda_{IM_0}} \quad (1)$$

In Eq. (1) I is an indicator function that equals 1 if IM is larger than IM_0 for a given distance r, magnitude m, and ε; n is the number of seismic sources relevant for the hazard at the site, ν_i is the earthquake occurrence probability for the fault i; $f\left(m,r,\varepsilon\right)$ is the joint PDF of {M, R, ε} and λ_{IM_0} is the hazard for IM_0.

Because disaggregation results may change with the considered spectral period, in this work DEs are computed for two different spectral accelerations[3], Sa, at 0s (i.e., peak ground acceleration or PGA), and 1.0s in order to account for short and moderate period regions of the response spectrum.

To perform disaggregation it is required first to compute hazard for the two IMs considered. Both PSHA and disaggregation analyses were performed by a computer program specifically

[2] In principle other source features may considered in disaggregation (e.g., faulting style, hanging/foot wall, etc) yet their relevance with respect to engineering practice is not fully proven to date.
[3] INGV also indirectly provides data about the seismic scenarios mostly contributing to the hazard, but only referring to peak ground acceleration.

developed and also used in [9]. The whole country was discretized using the same grid of about 10760 points adopted by INGV and, therefore, by the Italian seismic code. The seismogenic sources are that of [11], adopted by INGV (Figure 1), while seismic parameters of each zone are those used by Barani et al. [12][4], Table 1.

According to Ambraseys et al. [14], which is the GMPE considered: magnitude is that of surface waves (Ms). All the analyses refer to rock or stiff soil conditions.

Assuming a uniform epicenter distribution in each seismogenic zones, epicentral distance distribution is the appropriate one; because the used GMPE refers to closest horizontal distance to the surface projection of the fault plane (R_{jb}) as defined by Joyner and Boore [15], the former was converted into the latter via the linear relationship given in [16]. Distance applicability limits of the GMPE were respected and contributions to hazard distant more than 200km from the site were neglected in computations, which considered four return periods corresponding to the reference limit states for civil and strategic structures (i.e., 50, 475, 975 and 2475 years).

It is also to mention that no background seismicity was included, this is consistent with the INGV assumptions, as no significant influence on hazard was found; see [17] for details.

2.1 PGA and Sa(1s) hazards

Hazard curves were computed using thirty values of the IMs equally distributed between 0.001g and 1.5g. Computed hazard maps for the two spectral ordinates and the four return periods are reported in Figure 2 and Figure 3. In order to validate these results INGV data are assumed to be the benchmark, and with respect to them hazard values computed in this study are in good general agreement. In fact, INGV considered an extended logic-tree accounting for two earthquake catalogs, two different seismic rate models and maximum magnitude estimations, and four attenuation models [17]. This explains some differences found: in particular PGA differs from INGV mostly for sites enclosed into zones 927 and 935, while Sa(1s) for zones 905 and 935 (refer

[4] An erratum [13] to this reference reports b values for zones 903, 920 and 922 different, different with respect to those considered in this study. However, given differences between correct and incorrect values and geographical location of zones, it is believed that changing these parameters should have minor influence on results presented in the following.

to http://esse1.mi.ingv.it/ for comparisons).

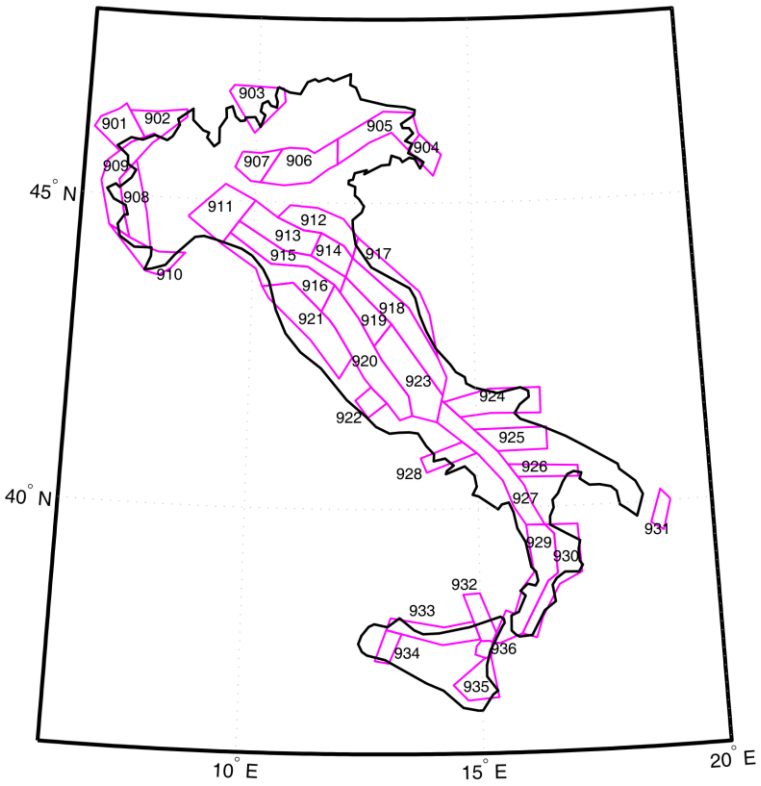

Figure 1. Seismogenetic zones for Italy according to [11].

Table 1. Characterization of seismic sources according to Barani et al. [12]. For each zone it is provided: minimum (M_{min}) and maximum magnitude (M_{max}); annual rate of earthquake occurrence above $M_{min,}$ (υ); and negative slope of Gutenberg-Richter relationship (b).

Zone	M_{min}	M_{max}	υ	b
901	4.3	5.8	0.045	1.133
902	4.3	6.1	0.103	0.935
903	4.3	5.8	0.117	1.786
904	4.3	5.5	0.050	0.939
905	4.3	6.6	0.316	0.853
906	4.3	6.6	0.135	1.092
907	4.3	5.8	0.065	1.396
908	4.3	5.5	0.140	1.408
909	4.3	5.5	0.055	0.972
910	4.3	6.4	0.085	0.788
911	4.3	5.5	0.050	1.242
912	4.3	6.1	0.091	1.004
913	4.3	5.8	0.204	1.204
914	4.3	5.8	0.183	1.093
915	4.3	6.6	0.311	1.083
916	4.3	5.5	0.089	1.503
917	4.3	6.1	0.121	0.794
918	4.3	6.4	0.217	0.840
919	4.3	6.4	0.242	0.875
920	4.3	5.5	0.317	1.676
921	4.3	5.8	0.298	1.409
922	4.3	5.2	0.090	1.436
923	4.3	7.3	0.645	0.802
924	4.3	7.0	0.192	0.945
925	4.3	7.0	0.071	0.508
926	4.3	5.8	0.061	1.017
927	4.3	7.3	0.362	0.557
928	4.3	5.8	0.054	1.056
929	4.3	7.6	0.394	0.676
930	4.3	6.6	0.146	0.715
931	4.3	7.0	0.045	0.490
932	4.3	6.1	0.118	0.847
933	4.3	6.1	0.172	1.160
934	4.3	6.1	0.043	0.778
935	4.3	7.6	0.090	0.609
936	3.7	5.2	0.448	1.219

Discrepancies derive mostly from the mentioned different hazard modeling, but analyzing results for sites in zones 905, it was also found a non negligible influence of the lumping of hazard curves in a certain number of IM values. In fact, computing PSHA again and assuming a finer discretization (60 points equally distributed between 0.001g and 1.5g), accordance with INGV

results is significantly improved; however, choice of thirty points was retained as a compromise that seems to provide trends of results that are generally acceptable and affordable for computing time demand.

Because the main object of the work is the definition of DEs, accordance with INGV disaggregation data was considered more important than that related to hazard data. Validation refers to PGA (disaggregation of Sa(1s) is not provided by INGV) and, again, general consistency was found; some exceptions were identified for some low seismicity sites (also in this case increasing IM discretization may reduce the gap). While details cannot be reported here for the sake of brevity, the reader is referred to Chioccarelli [18] for further information.

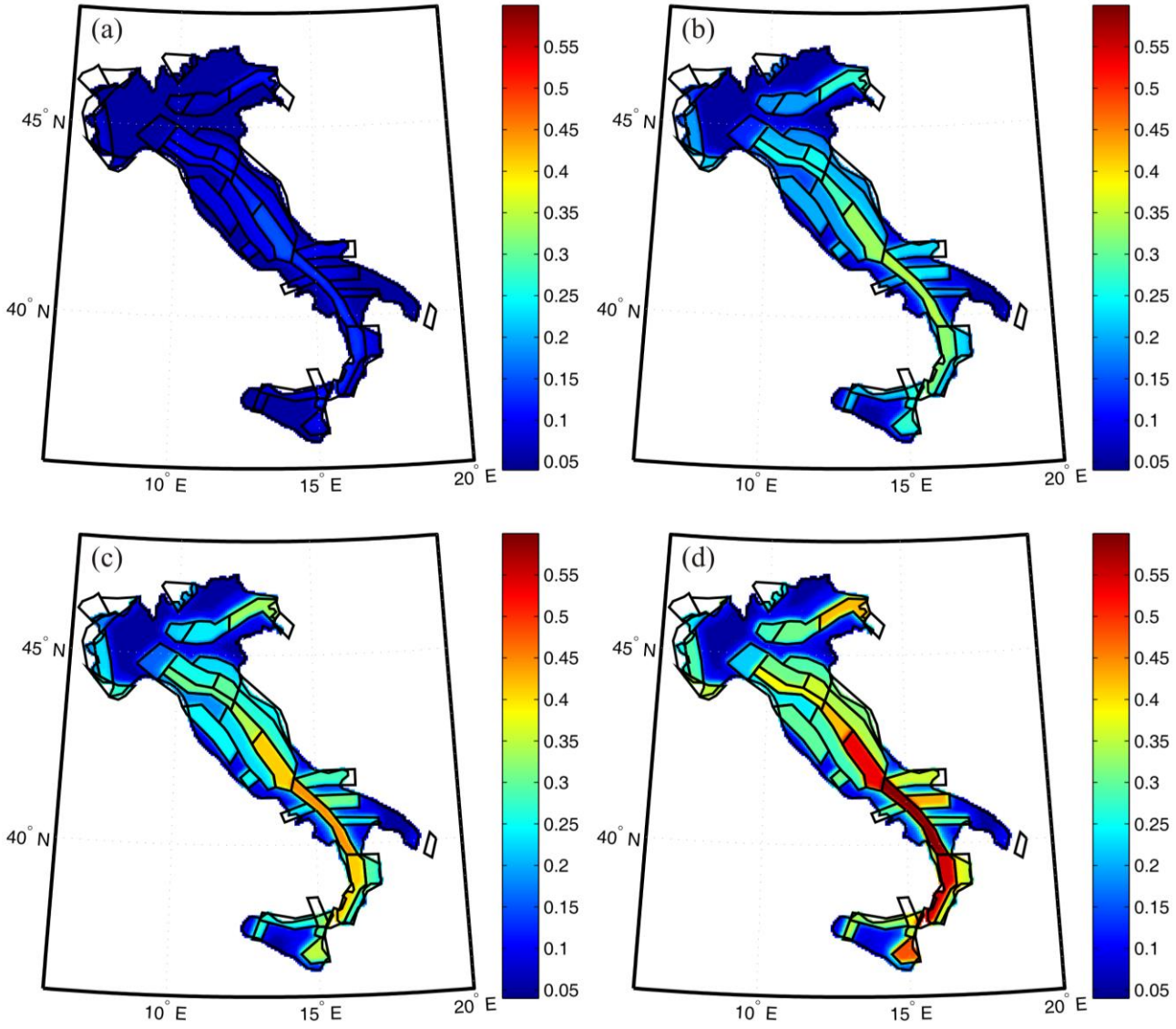

Figure 2. Hazard maps of PGA, in fractions of g, for Tr equal to 50yr (a), 475yr (b), 975yr (c) and 2475yr (d).

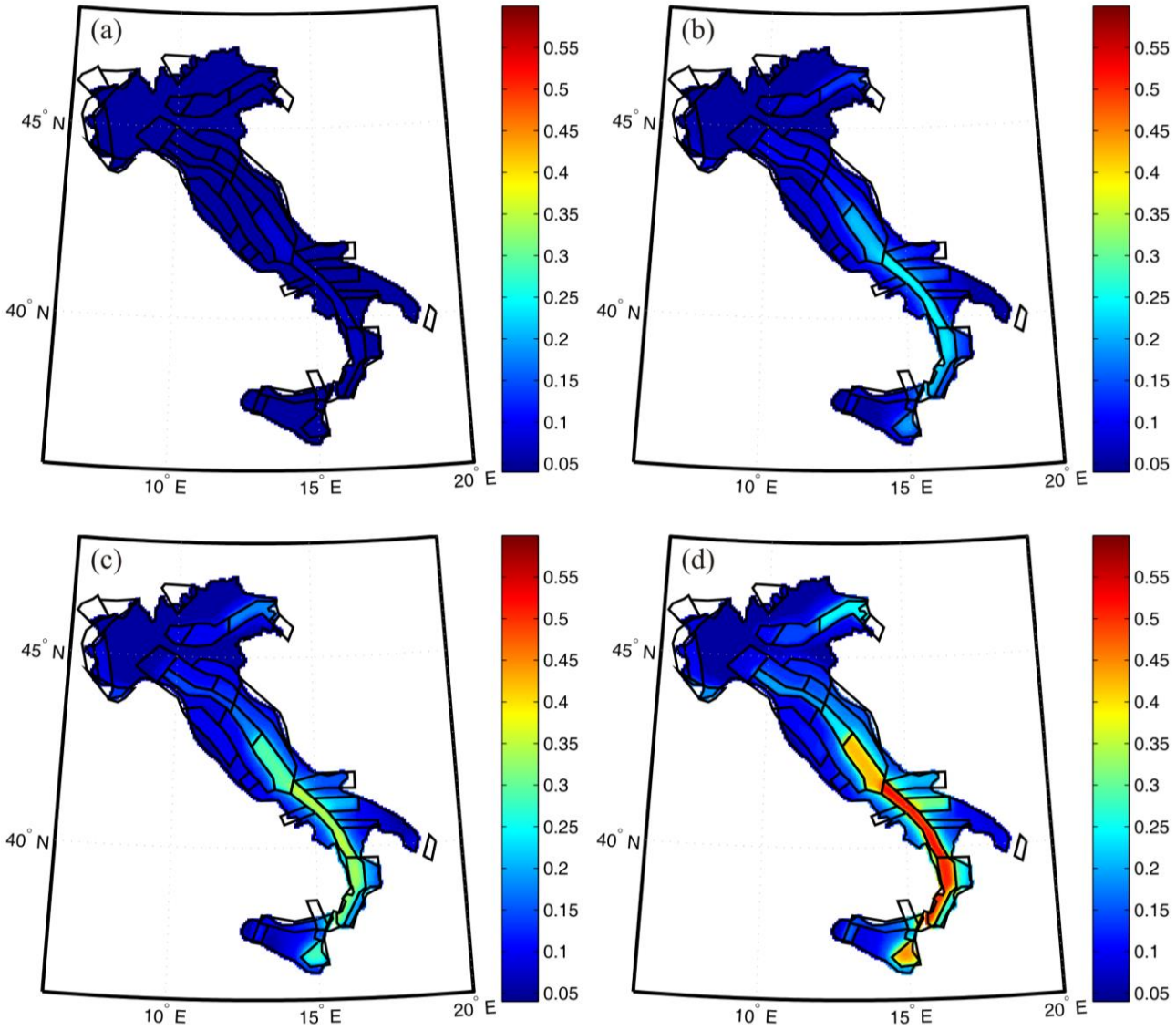

Figure 3. Hazard maps of Sa(1s), in fractions of g, for Tr equal to 50yr (a), 475yr (b), 975yr (c) and 2475yr (d).

3. Identifying and mapping design earthquakes

Disaggregation integral in Eq. (1) is computed numerically by the software using bins of 0.05, 1.0km and 0.5 for M, R and ε respectively (ε varies between -3 and +3). This means that the disaggregation PDF, which is continuous in principle, is rendered a discrete function.

Recalling that for each site, return period and spectral ordinate, disaggregation results in a four dimensional surface providing the contribution to hazard of M, R and ε variables, multiple DEs can be identified. Herein, the *first* DE is defined as the mode of the disaggregation PDF; i.e., the vector {M*, R*, ε*} most frequently causing the exceedance of the IM threshold corresponding to the considered return period. Moreover, as extensively discussed in [9], because analyses show that

in many cases disaggregation PDF has more than a single mode significantly contributing to hazard, a *second* DE is defined as the second relative maximum of the $f\left(m,r,\varepsilon|IM>IM_0\right)$ distribution. Herein, to ensure the second DE to be of practical relevance, two additional (arbitrary) conditions were imposed with respect to [9]:

1. the second mode is identified as an event different from the first DE if the two differ by 5.0km in distance and/or 0.25 in magnitude;
2. the second DE is considered as such if the second mode of the disaggregation PDF gives a contribution to hazard larger than 10^{-4}.

See next section for analysis of significance of DEs identified via these criteria.

Maps of DEs are reported in Figure 4 to Figure 11 (R in km), in which it is possible to identify some general trends: (i) the first mode corresponds to an earthquake caused by the closer source (or the source the site is enclosed into) and with low-to-moderate magnitude, (ii) the second mode accounts for the influence of the more distant zones usually with larger magnitude, and (iii) moving from PGA to Sa, the number of sites with two DEs increases. As consequence of (ii) and (iii), it can be inferred that the influence of more distant zones is higher for Sa(1s) than for PGA.

Each of these conclusions will be examined further and explained in the following via case studies referring to specific sites. It may be anticipated that, of course, all disaggregation results can be motivated looking at GMPE and seismogenic model adopted. However, because most of the ordinary GMPEs show similar dependencies with respect to magnitude and distance, while several different options may underlie modeling of seismic sources, it is believed that changing GMPE may change the results without losing general trends, conversely, changing the seismic source model (especially the geometrical shape of source zones) can alter results dramatically.

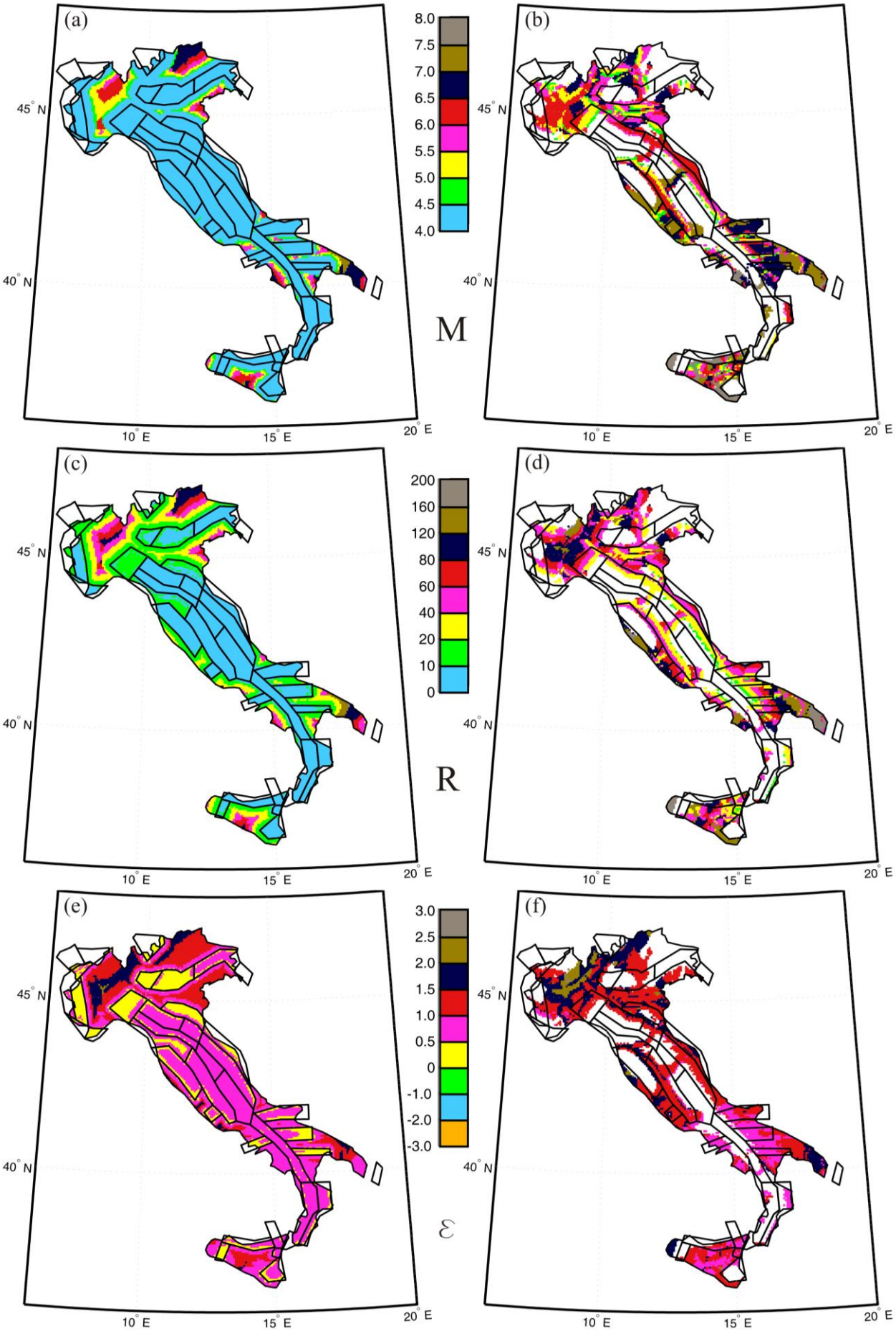

Figure 4. First (left) and second (right) modal values for PGA and Tr = 50yr.

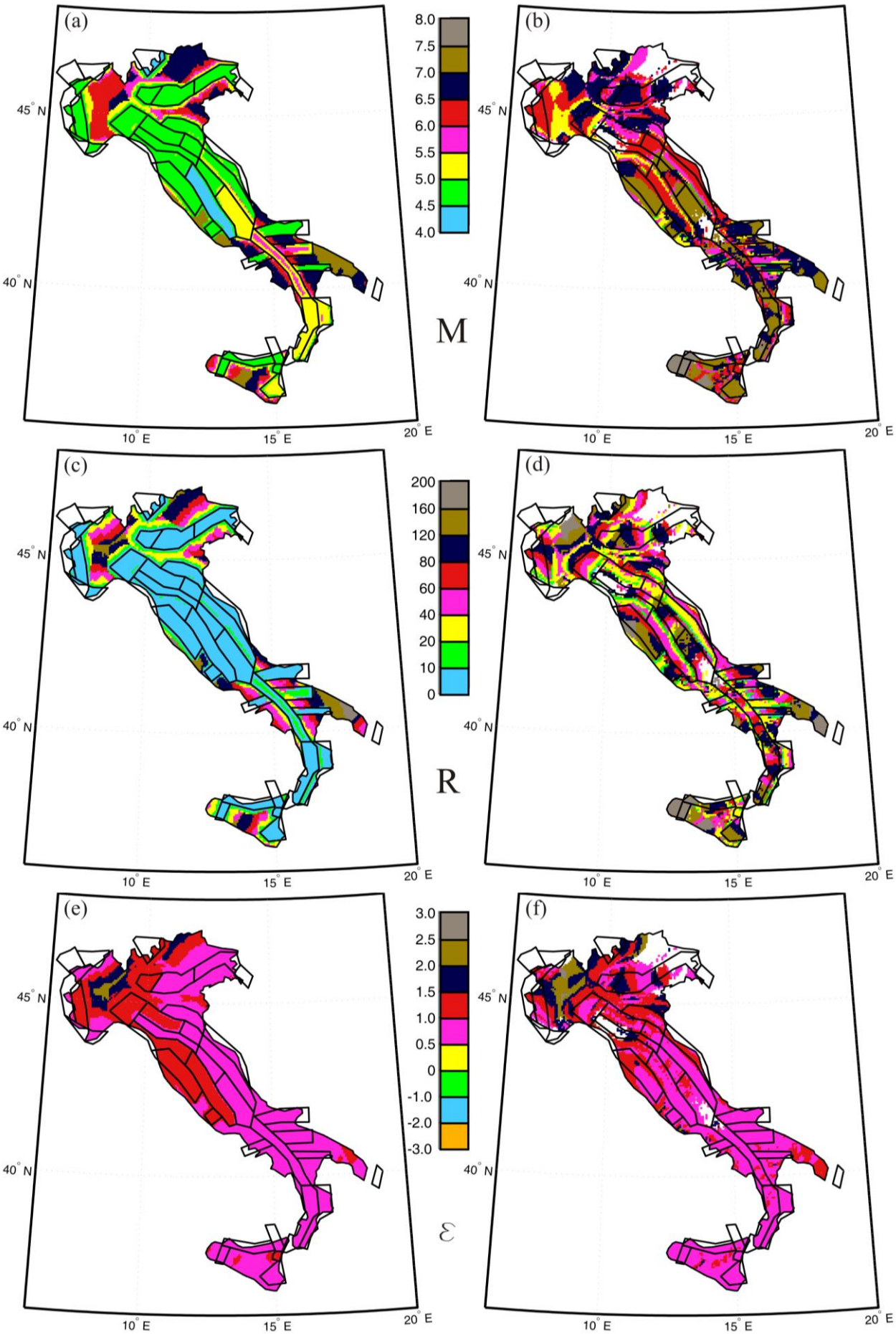

Figure 5. First (left) and second (right) modal values for Sa(1s) and Tr = 50yr

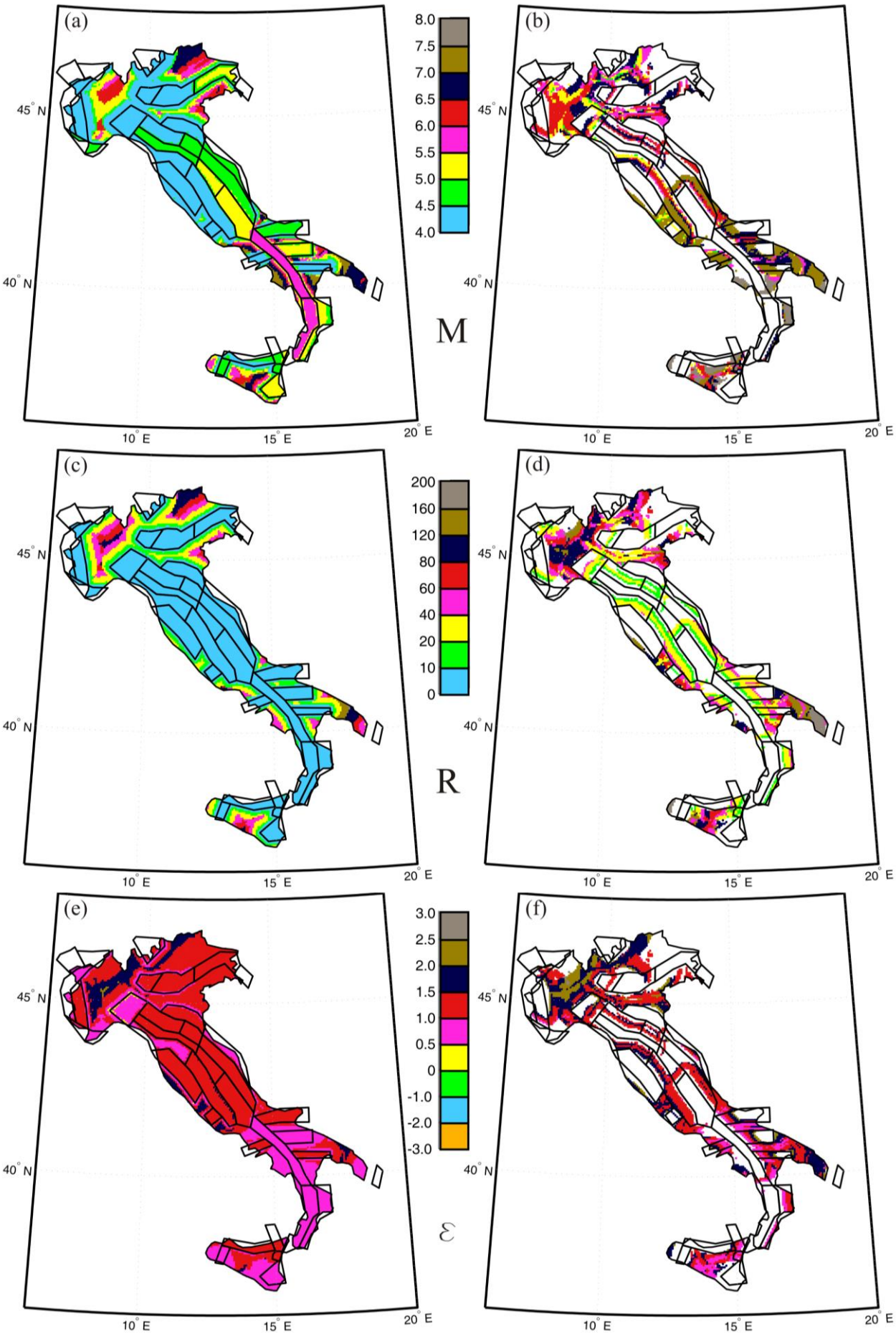

Figure 6. First (left) and second (right) modal values for PGA and Tr = 475yr.

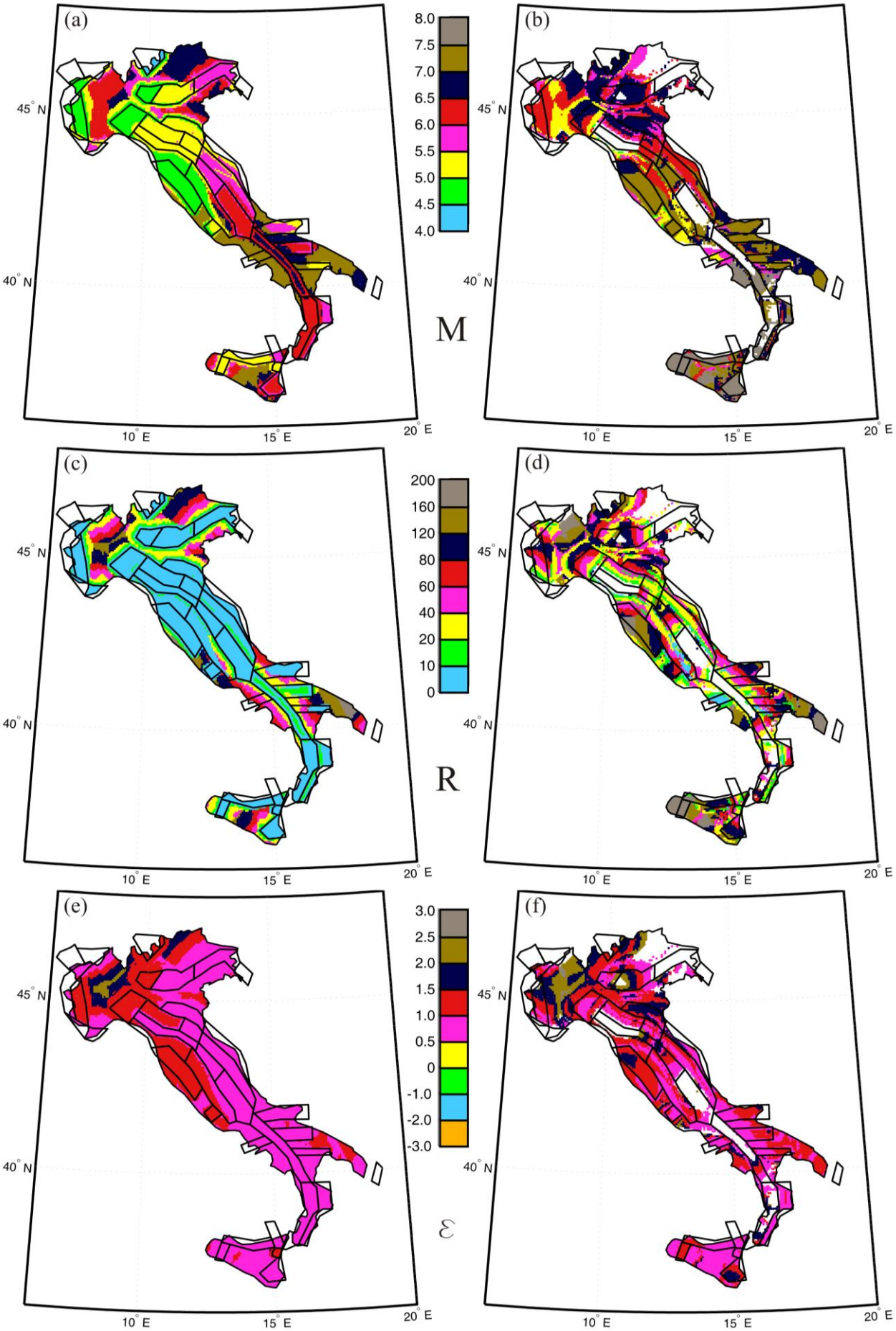

Figure 7. First (left) and second (right) modal values for Sa(1s) and Tr = 475yr.

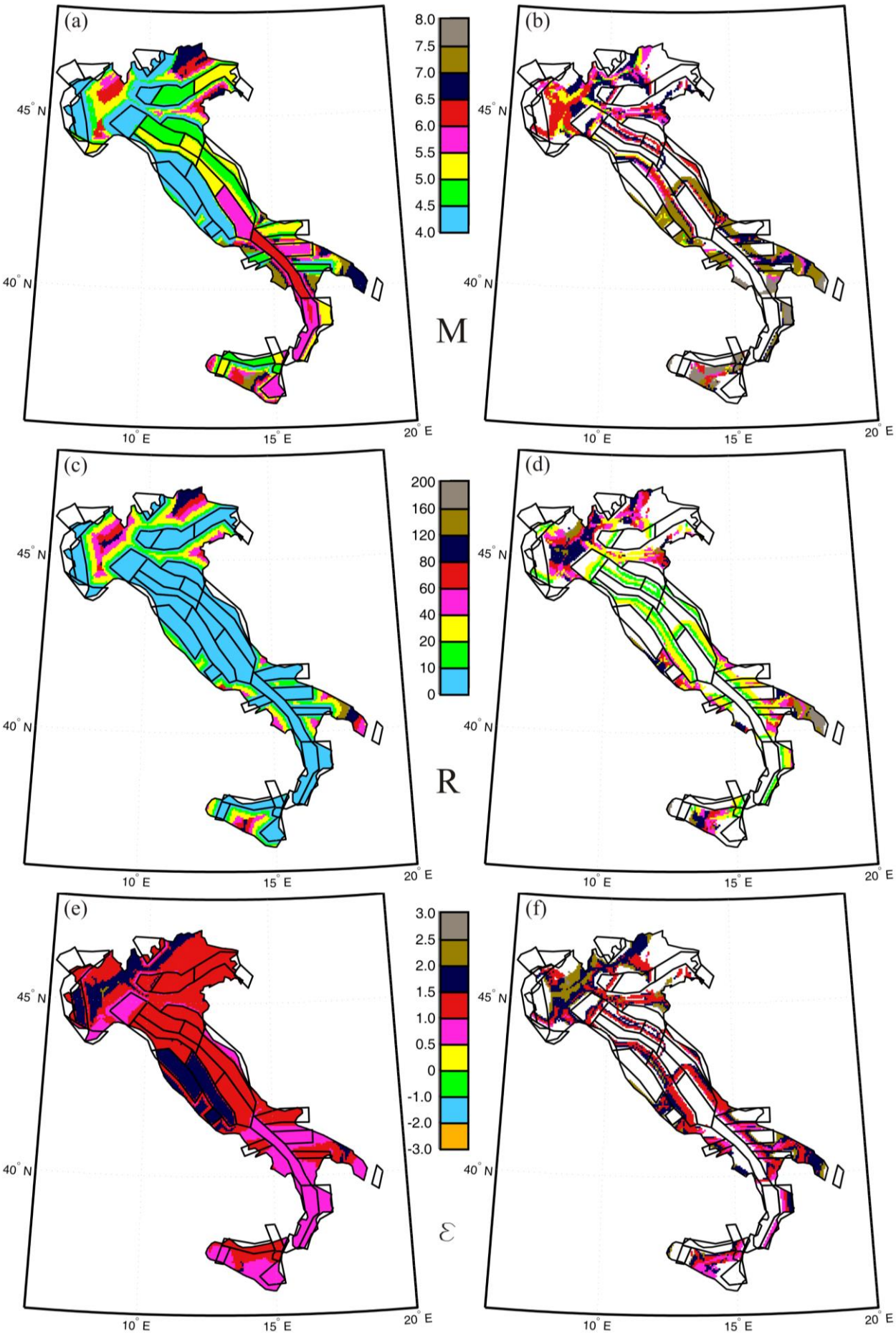

Figure 8. First (left) and second (right) modal values for PGA and Tr = 975yr.

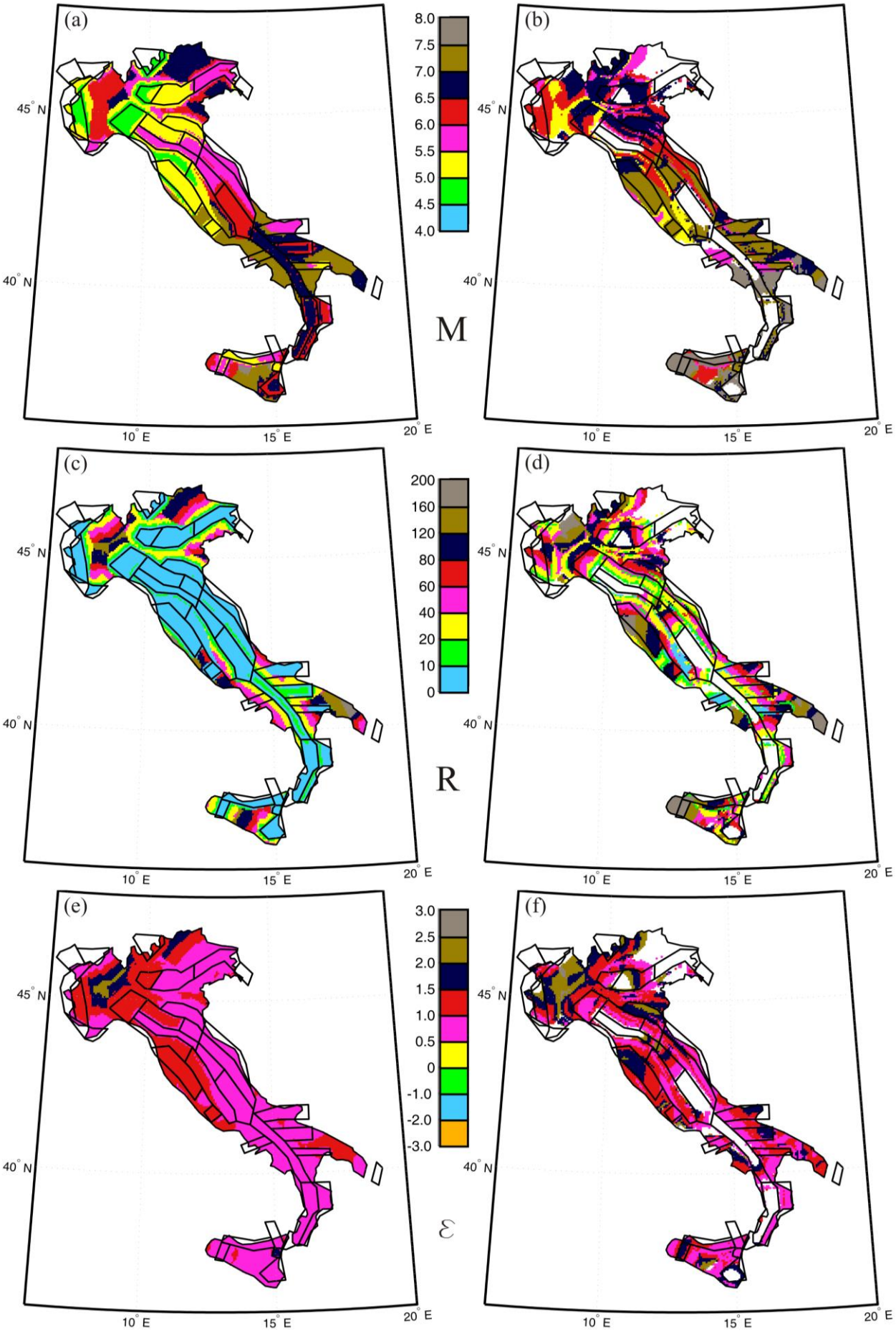

Figure 9. First (left) and second (right) modal values for Sa(1s) and Tr = 975yr.

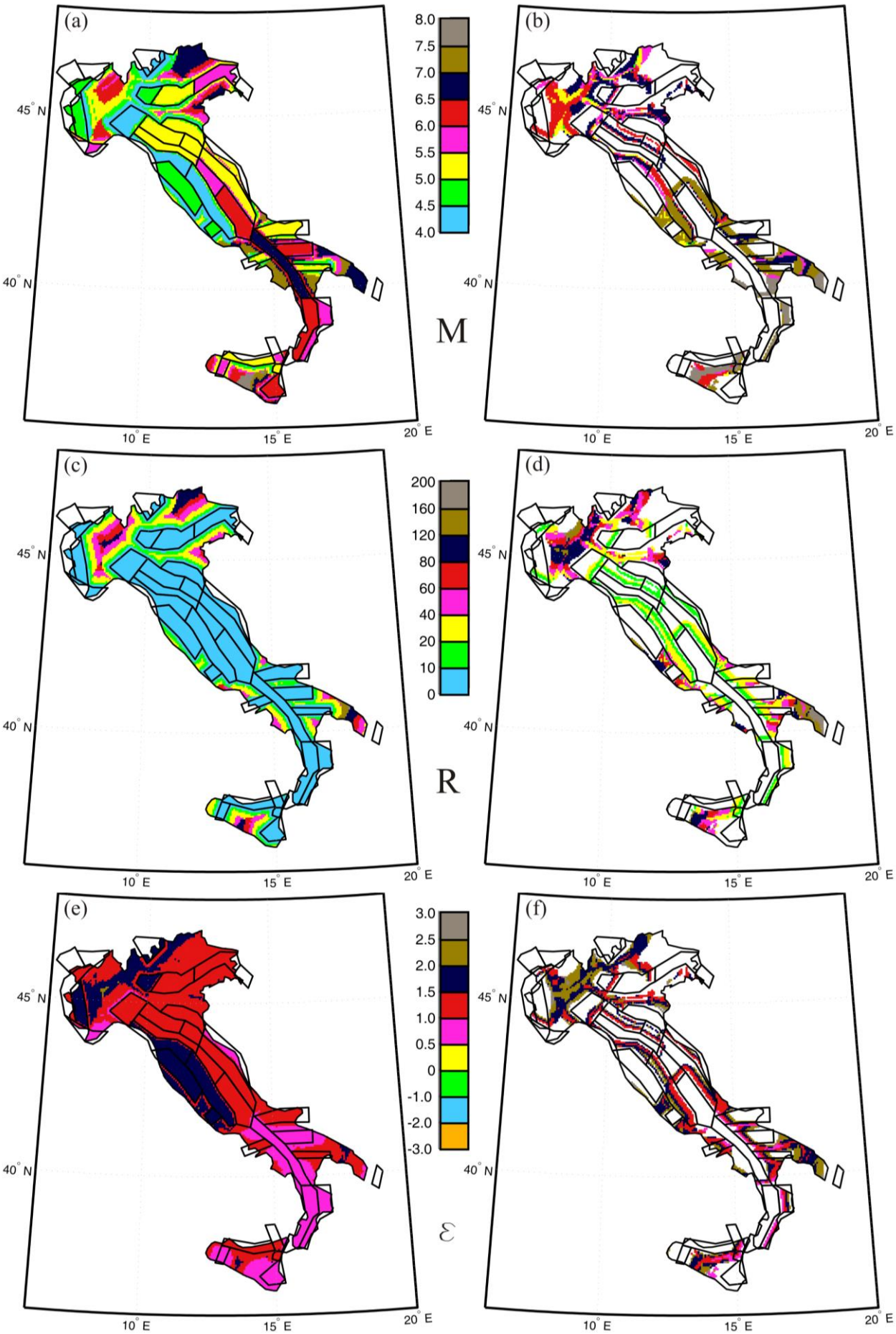

Figure 10. First (left) and second (right) modal values for PGA and Tr = 2475yr.

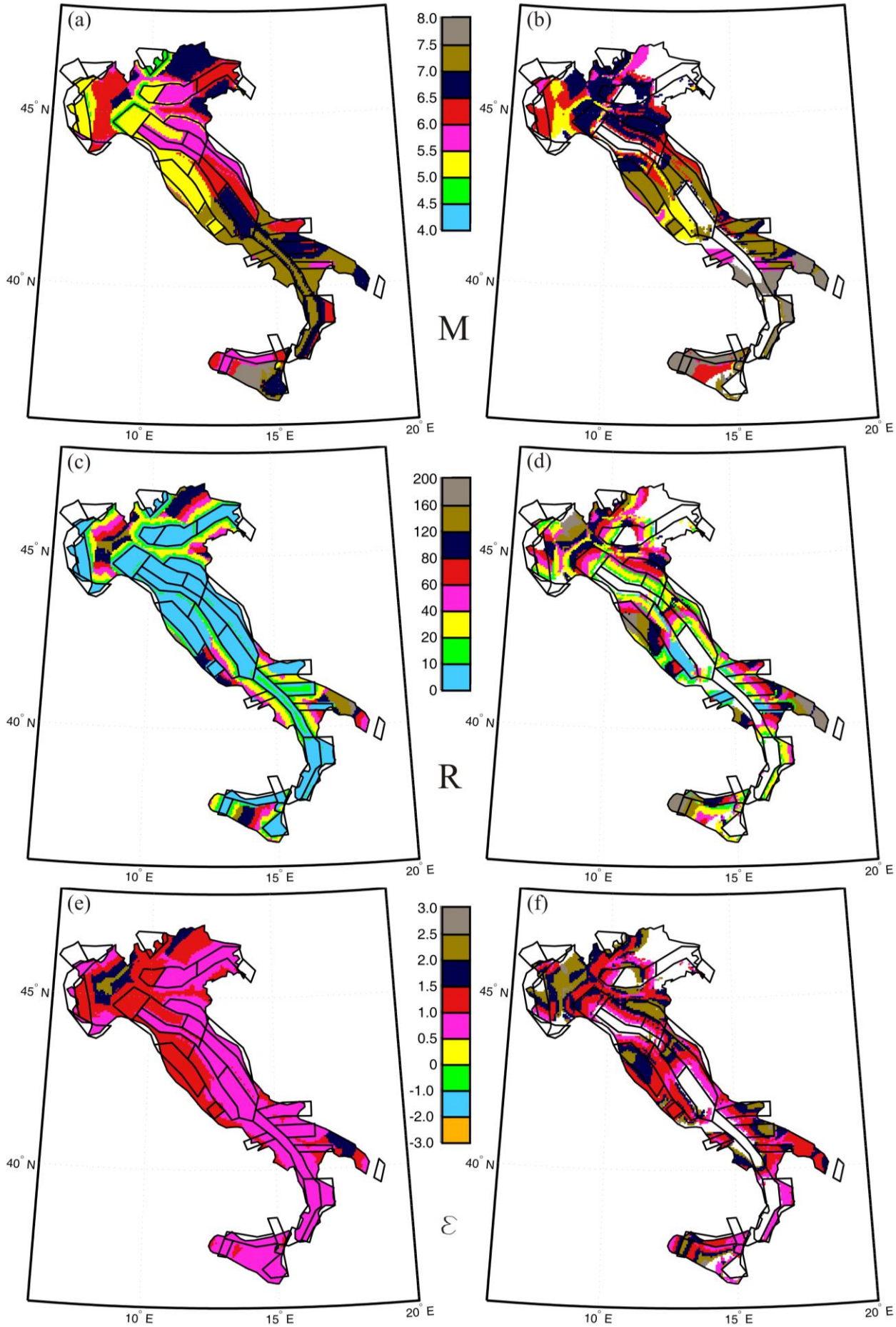

Figure 11. First (left) and second (right) modal values of ε for Sa(1s) and Tr = 2475yr.

3.1 Implications of disaggregation modes as design scenarios

3.1.1 Significance based on contributions to hazard

Identification of DEs by modal values, as shown in the maps above, is useful for the practical use of disaggregation results. However, in some cases they cannot be representative enough of the whole disaggregation distribution. Examples of critical cases are reported below while in next sections specific sites are studied.

Because many different earthquakes can affect the hazard at a site, disaggregation may show an especially flat shape. When this condition occurs, modal values can be comparatively less representative to determine design scenarios. An example is the site of Campobasso (14.668° E, 41.561° N) considered here for Sa(1s) and Tr equal to 50yr. Location and disaggregation distribution[5] are shown in Figure 12 (hereafter, considered sites are indicated in the maps by triangles) . According to the procedure described in previous section first and second DEs are {6.5km; 4.93, 0.5} and {13.5km; 5.53, 0.5} respectively in terms of distance, magnitude and ε and the distribution does not seem to have a third significant mode but it is clear that also large distance and magnitude values give a non-negligible hazard contribution.

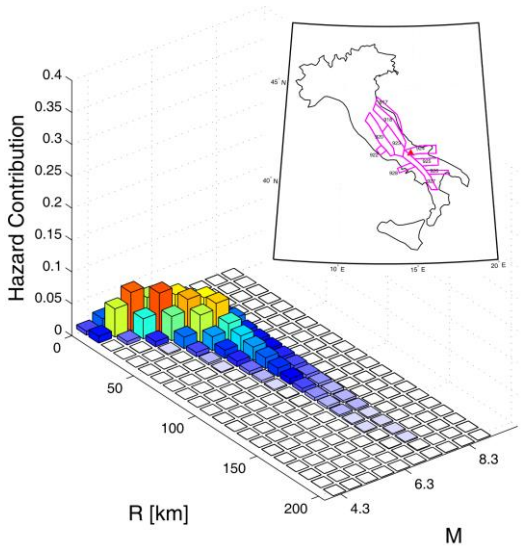

Figure 12. Disaggregation Sa(1s) hazard with Tr = 50yr in Campobasso.

[5] Hereafter for all the site-specific cases, disaggregation surfaces will be shown as tridimensional; i.e., after marginalization of $f\left(m,r,\varepsilon\middle|IM>IM_0\right)$ with respect to ε so to obtain $f\left(m,r\middle|IM>IM_0\right)=\int_{\varepsilon} f\left(m,r,\varepsilon\middle|IM>IM_0\right)d\varepsilon$. Despite this pictorial choice, modal values presented are always computed on the four-dimensional disaggregation surface.

Referring to identification of the second mode, the 10^{-4} minimum contribution threshold has been chosen looking at disaggregation for several sites, yet it is still arbitrary and PDFs can have different shapes in a way that a unique assumption may not satisfy all the cases. As a site-specific example, the Caltanissetta city (14.18° E, 37.33° N) is considered. The disaggregation of Tr = 50yr PGA hazard for this location is reported in Figure 13a. First and second DEs are identified in terms of R and M as {54.5km, 6.08, 1.0} and {144.5km, 7.58, 1.0}, while associated probabilities are $5.6 \cdot 10^{-3}$ and $5.7 \cdot 10^{-4}$, respectively. Considering a second DE, it seems to be a reasonable choice because several M and R bins give low but non-negligible contribution to hazard in a way that globally the second mode appears significant[6]. Conversely, looking at disaggregation for Tr = 475yr PGA hazard in Naples (14.191° E, 40.829° N), Figure 13b, the second mode {50.5km; 7.3, 1.50} has an hazard contribution[7] equal to $2.8 \cdot 10^{-4}$, but its contribution seems to be negligible because no other close bins have comparable associated probability.

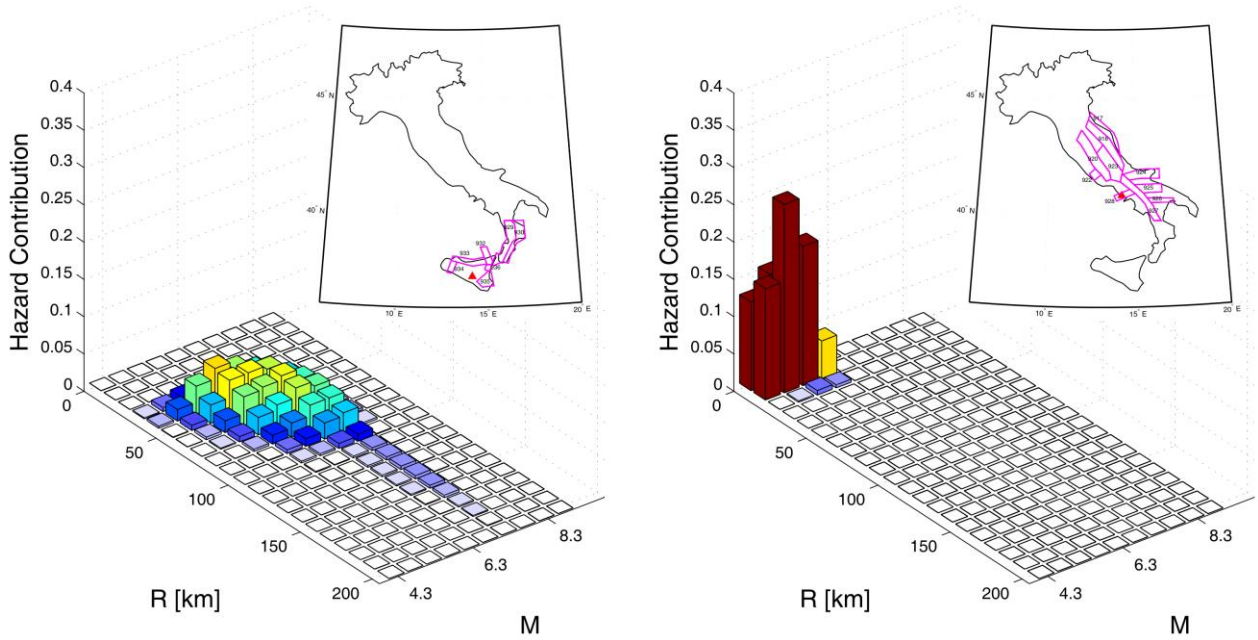

Figure 13. Cases of relevant (a) and negligible (b) second mode hazard contribution.

[6] Importance of magnitude and distance for engineering practice may refer, for example, to cyclic demand imposed to structures by ground motion; i.e., different earthquakes determining similar spectral ordinate may be different in duration if characterized by different M and R pairs [19].

[7] In the plots bins with contribution lower than $1.2 \cdot 10^{-3}$ are shown in white.

3.1.2 Significance based on spectral regions

Disaggregation of 1s spectral acceleration was considered representative of a response spectrum region of engineering interest. In fact, in this section hazard disaggregation for other structural periods is shown to assess the range in which 1.0s results can still be considered significant. The analyzed site is Viterbo (12.107° E, 42.426° N). In Figures 14 and 15 PDFs for Tr = 50yr and Tr = 2475yr are reported. For both return periods disaggregation for spectral acceleration at 4 structural periods is given: PGA, 0.5s, 1.0s, and 2.0s.

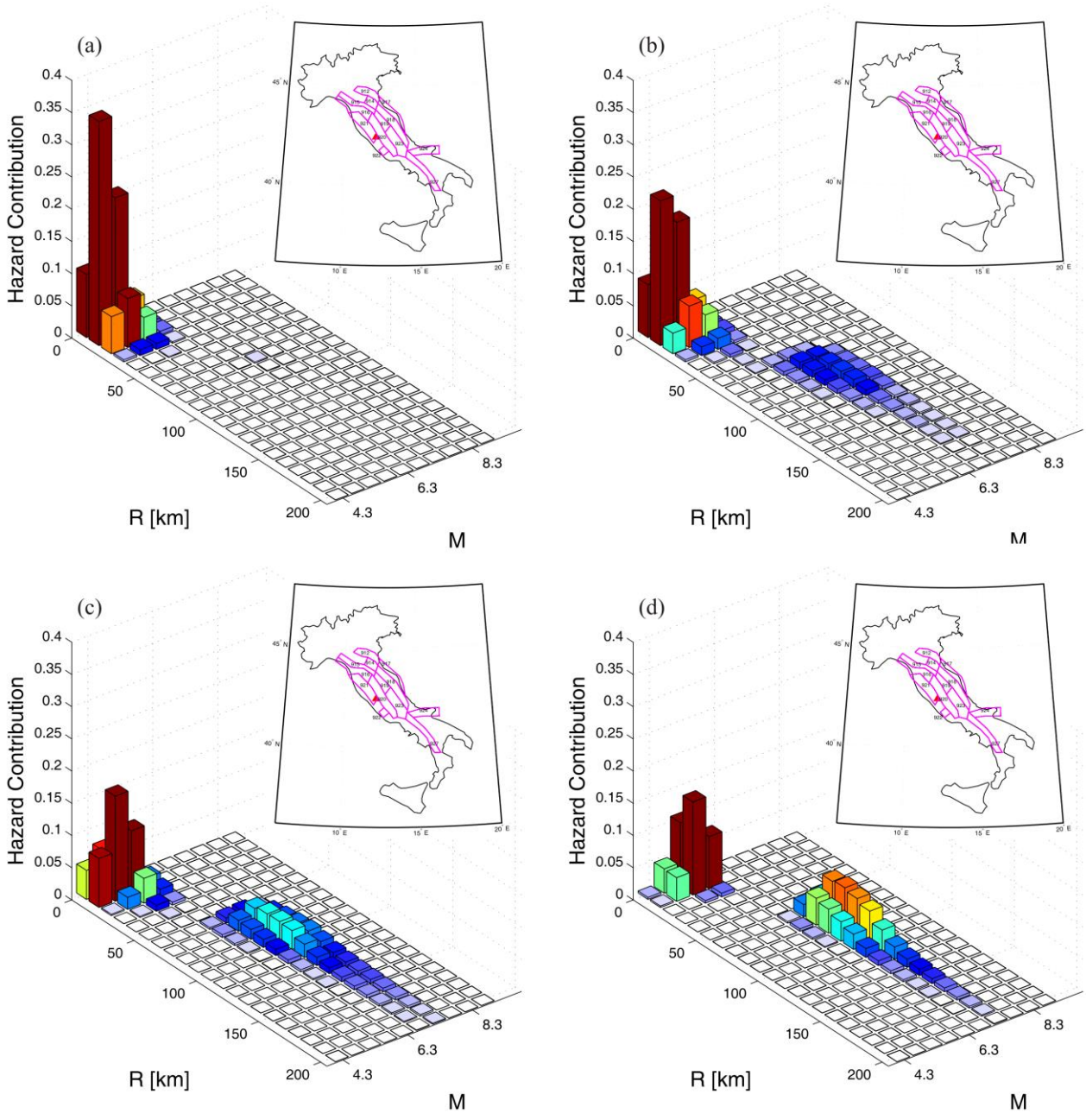

Figure 14. Disaggregation for Viterbo and Tr = 50yr: PGA (a), T = 0.5s (b), T = 1.0s (c) and T = 2.0s (d).

For Tr = 50yr, it appears, as expected, that results for T = 2.0s are well represented by disaggregation for T = 1.0s, much better if compared to PGA. Also disaggregation for T = 0.5s seems to be better represented by T = 1.0s results with respect to PGA, because of a second mode more clearly appearing in the latter with respect to the former.

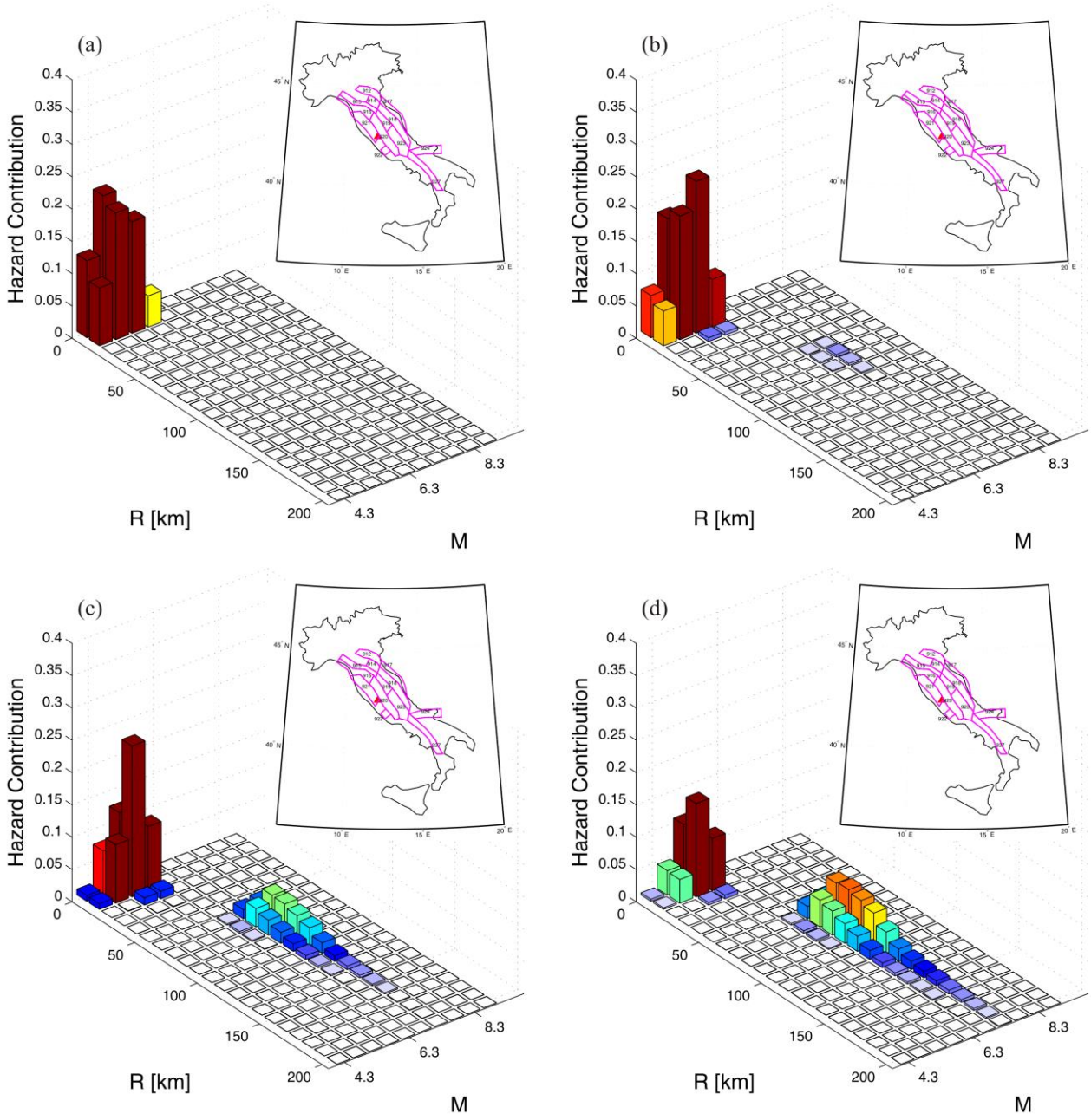

Figure 15. Disaggregation for Viterbo and Tr = 2475yr: PGA(a), T = 0.5s (b), T = 1.0s (c) and T = 2.0s (d).

Although less evident, the same conclusion holds for Tr = 2475yr because the contribution of the second mode (evident for T = 1s) is also visible for T = 0.5s. In particular, the second DE is

{67.5km, 7.28, 1.5} and gives a contribution to hazard equal to $1.2 \cdot 10^{-3}$, which is significant according to the threshold conventionally established in the previous section. Therefore, disaggregation of PGA hazard seems representative for structures with fundamental period below 0.5s. In all other cases, disaggregation for Sa(1s) is a more rational choice.

It is to note finally the increasing contribution to hazard of the second mode if the spectral ordinate in which the hazard is disaggregated corresponds to a longer period, this is systematic and explained in section 4.2.

4. One, two, or more modes?

From the DEs maps given above, it appears that the second mode of disaggregation PDFs is not always identified (white regions in the maps) and that disaggregation is unimodal within, or around, specific seismic source zones. In fact, if a site is enclosed or close to a seismic source zone with *high seismicity* (in terms a of a combination of magnitude interval, annual rate of earthquake and *b*-value of Gutenberg-Richter) relatively to surrounding zones, the stronger zone dominates the hazard for the site. As a consequence, contributions to hazard will be concentrated in a relatively narrow M and R domain whose limits generally correspond to the minimum and maximum values of magnitude and distance of the zone borders from the site. For these cases, given the return period and the spectral ordinate of interest, the disaggregation PDF is unimodal and, therefore, characterized by a single DE.

One of these sites is represented by L'Aquila (13.396° E, 42.365° N) whose disaggregation is reported here for a return period equal to 975yr (Figure 16) along with zones considered in its hazard computation. The site is enclosed in zone 923 characterized by M_{max} equal to 7.3, annual rate of earthquake occurrence (υ) equal to 0.645, and a *b*-value of 0.802 (Table 1). All the closer zones (918, 919, 920) have lower maximum magnitude, lower υ, and higher *b*. These numbers suggest that zone 923 has the higher seismicity and, therefore, unimodal disaggregation is expected, as shown.

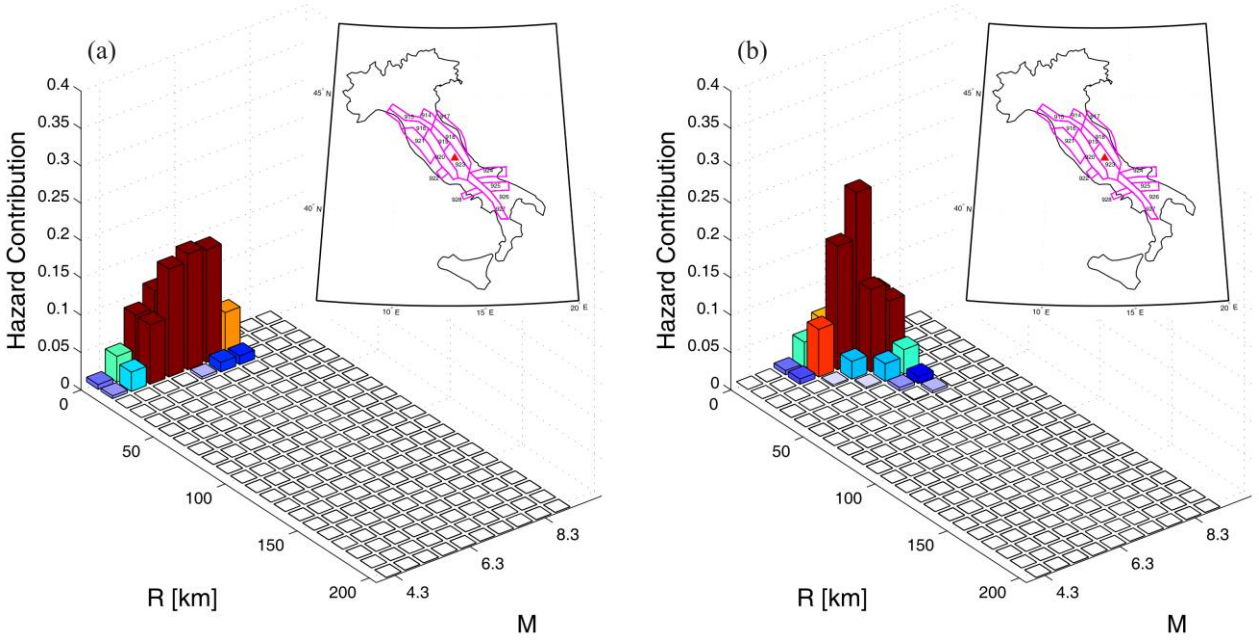

Figure 16. Disaggregation results for L'Aquila, Tr = 975, PGA (a) and 1s (b).

Conversely, maps indicate at least two different DEs for many sites. An example is the city of Bari (16.879° E, 41.113° N) in southern Italy. Figure 17a shows disaggregation for PGA hazard at Tr = 50yr, while that for Sa(1s) and Tr = 475yr is reported in Figure 17b. Both disaggregations have two significant modes (it will be discussed in the next sections how dominant earthquakes change with the structural period and with return period, at this stage, however, it is worthwhile to anticipate that bimodal cases are more easily available for Sa(1s) than for PGA); PDF for PGA provides first and second modal values in terms of R, M and ε equal to {35.5km; 5.8; 0.5} and {125.5km; 7.3; 1.0} respectively. First and second DE for Sa(1s) are {132.5km; 7.3; 1.0} and {35.5km; 6.7; 0.5} respectively[8]. Closer zones to the site are 924, 925 926 and 927. Zone 925 is the closest one and it determines the first DE. Zones 924 and 926 have approximately the same distance to the site, but zone 924 has higher seismicity in terms of M_{max} and υ (see Table 1). Zone 927 is slightly more distant, but its seismic parameters are significantly higher than those associated to all the other zones considered here. In fact, the maximum magnitude is 7.3 and υ is almost twice of the maximum among other zones. Zone 927 is the cause of a relevant second DE.

[8] Looking at Figure 17b, it seems the first DE is that corresponding to the second mode. This is an effect of marginalization with respect to ε required to display an otherwise four dimensional PDF on which the modes are actually identified as discussed earlier.

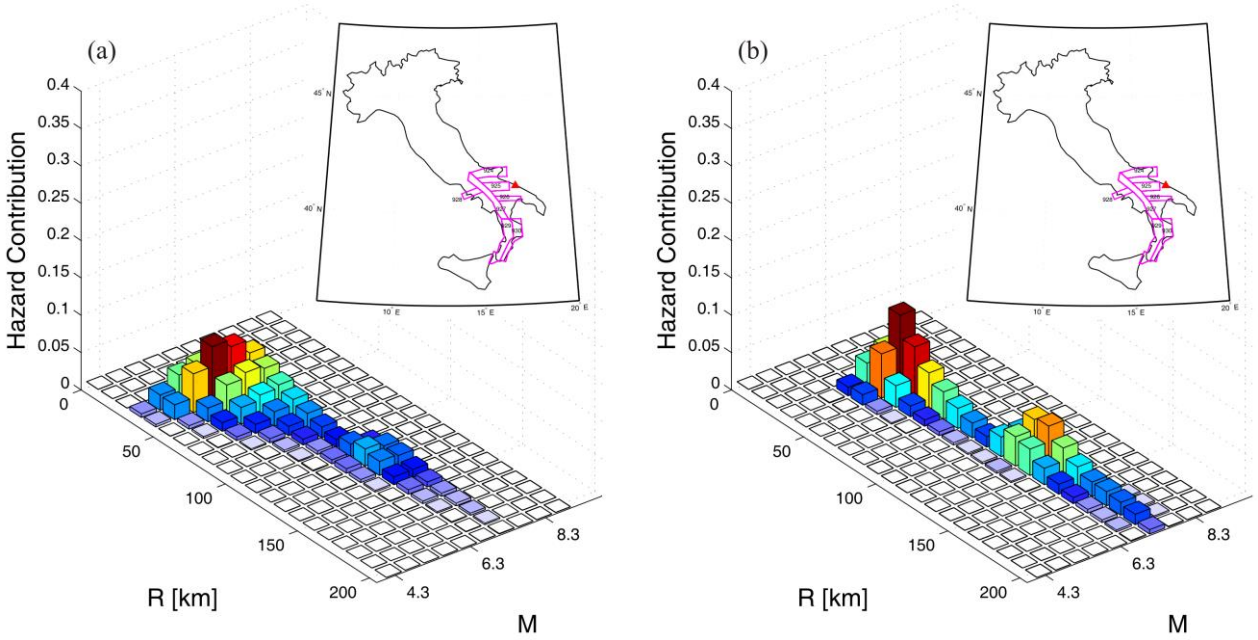

Figure 17. Disaggregation results for Bari, Tr = 50yr, PGA (a) and Tr = 475yr, Sa(1s) (b).

For the same reasons behind a bimodal PDF, it is possible a site has even more DEs. An example is Ancona (13.506° E, 43.589° N) for which Tr equal to 50yr is considered (Figure 18). Sa(1s) hazard disaggregation shows three modes: the first two modes in terms of R, M and ε are {7.5km; 5.0; 0.5} and {33.5km; 6.2; 0.5} respectively.

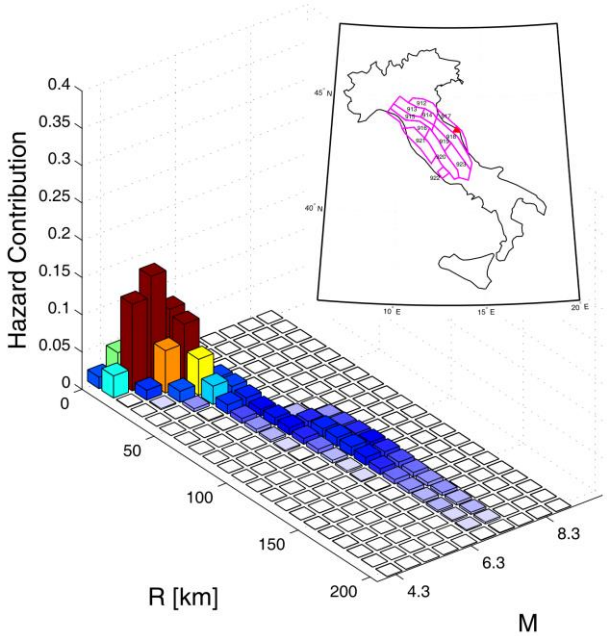

Figure 18. Disaggregation results for Ancona, Sa(1s) and Tr = 50yr (b).

Marginalization on ε, proximity of the two modal values and bins representation make the two

modes coincident in the plot. A third significant mode corresponds to R and M equal to 110km and 6.8 respectively. This indicates that multiple zones give comparable contribution to hazard. In fact, for this particular case zones 917 and 918 determine the first two modes (being the first zone closer and the second with slightly higher seismicity), while the more distant zone 923 has a strong seismicity and has non negligible influence on the hazard of the site (third mode).

Because the contribution of the third mode, if any, is expected to be minor, this study focused on the first two DEs.

4.2 Effect of structural characteristics on number and significance of DEs

Maps and examples above indicate that disaggregation results can change significantly with the considered structural period the spectral ordinate refers to. This conclusion was anticipated looking at DEs maps and it is also shown for the specific site of Viterbo; see Figure 14 (a and c) and Figure 15 (a and c). The examples demonstrate that unimodal disaggregation results for PGA may become clearly bimodal for Sa(1s) with an higher magnitude and distance contribution to hazard. This is because of the GMPE. Indeed, for a fixed site and return period, variations of dominating earthquakes for different spectral ordinates can only depend on the used prediction equation (see also section 5). In particular, high frequency waves are attenuated faster with distance and therefore it is expected that spectral ordinates associated to longer periods (1.0s in this case) are more affected by distant events with respect to PGA. In other words, distant zones with negligible influence on PGA hazard, can show non-negligible effects on the Sa(1s) hazard at the same site. As a consequence, design scenarios based on PGA disaggregation can be potentially misleading for moderate-to-long fundamental periods as also discussed in [9].

5. Scenarios and Return Periods

An interesting result, which may not be inferred directly from DEs maps is that, for the most of sites featuring more than one mode, increasing the return period of the acceleration being disaggregated, the contribution of the first mode (the close-moderate earthquake) increases with respect to the

second mode. See, for example, San Severo (15.377° E, 41.687° N), whose disaggregation results for return periods equal to 50yr and 2475yr are reported in Figure 19 for both spectral ordinates considered. The influence of return period on the significance of the first mode is visible for both PGA and Sa(1s), although for PGA the effect is less evident because, as already discussed, more distant zones have lower influence on hazard with respect to Sa(1s) hazard.

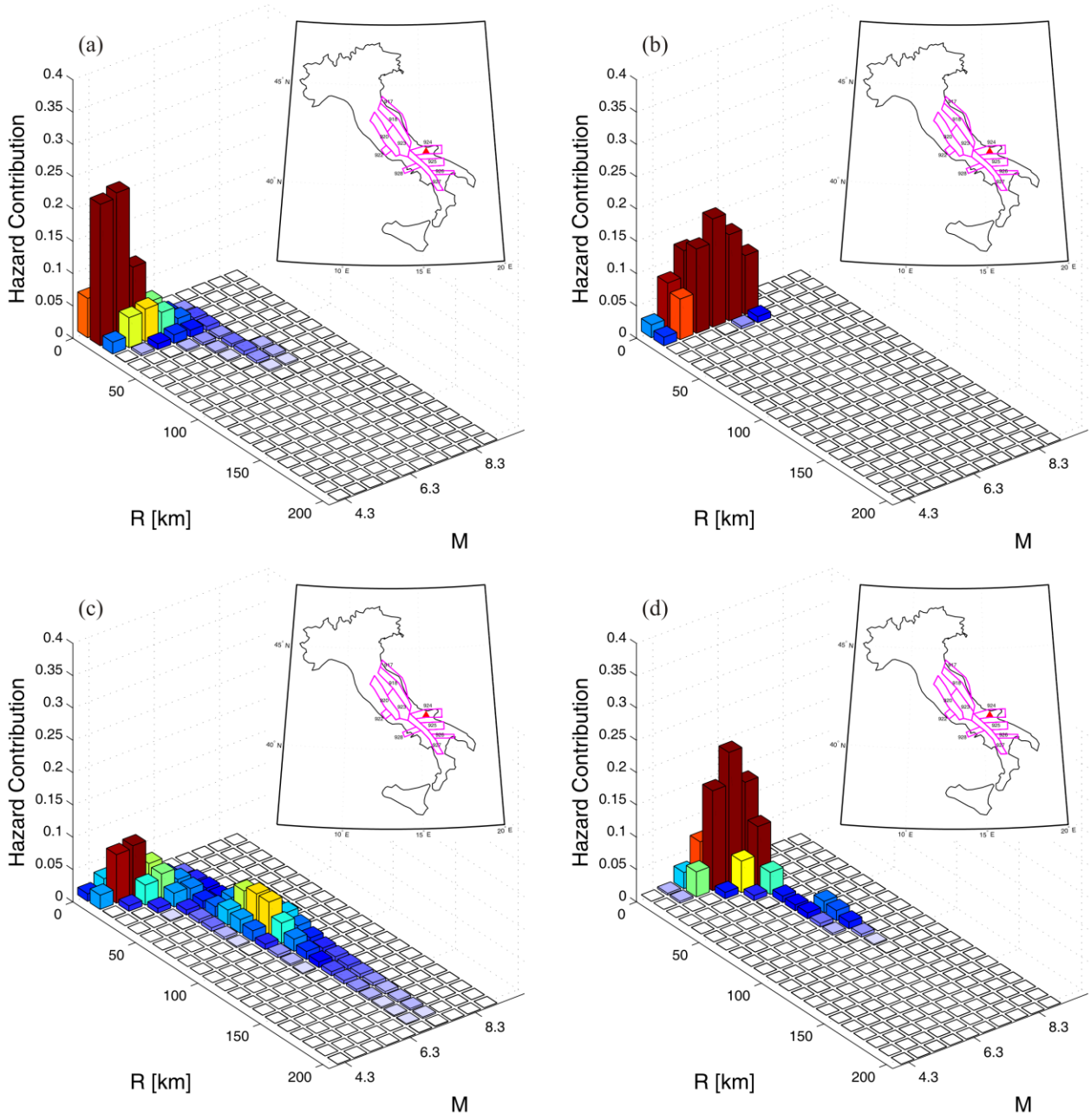

Figure 19. Disaggregation results for San Severo at PGA for Tr = 50yr (a) and 2475yr (b) and at Sa(1s) for Tr = 50yr (c) and 2475yr (d).

In order to demonstrate this trend of DEs' contributions to hazard (HC) with respect to Tr, it may be

useful to consider an extremely simple ideal case of a site affected by two source zones: Z_1 and Z_2 generating individual (characteristic) earthquakes $\{M_1,R_1\}$ and $\{M_2,R_2\}$ respectively, Eq. (2) and Eq. (3):

$$HC_{Z_1} = \frac{\nu_{Z_1} \cdot f\left(IM > IM_0 \middle| M_1, R_1\right)}{\lambda_{IM_0}} \tag{2}$$

$$HC_{Z_2} = \frac{\nu_{Z_2} \cdot f\left(IM > IM_0 \middle| M_2, R_2\right)}{\lambda_{IM_0}} \tag{3}$$

λ_{IM_0} is a marginal probability and it doesn't depend on the considered zone; ν_Z are the rates of occurrence of earthquakes for the two zones and $f\left(IM > IM_0 \middle| m,r\right)$ depends on the GMPE. Comparison of hazard contribution of the zones can be investigated via the ratio in Eq. (4).

$$\frac{HC_{Z_1}}{HC_{Z_2}} = \frac{f\left(IM > IM_0 \middle| M_1, R_1\right)}{f\left(IM > IM_0 \middle| M_2, R_2\right)} \frac{\nu_{Z_1}}{\nu_{Z_2}} \tag{4}$$

For a given return period, the zone with the higher product of activity rate and GMPE terms provides the higher contribution to hazard. Increasing Tr, IM_0 increases and the ratio of probabilities given by GMPE determines all the relative variations of contributions.

An illustrative numerical example may be given considering the scheme of site and zones sketched in Figure 20a. Considering the Ambraseys et al. [14] GMPE, if M_1 and M_2 are assigned equal to 5 and 6.5 and using as R_1 and R_2 average distances of the two zones from the considered site (5km and 135km, respectively), the ratio of HC (Figure 20a) has a positive slope indicating that the contribution of Z_1 increases with the threshold (i.e., IM_0), and therefore increases if the return period is increased.

The reason for that is plotted in Figure 20b. In fact, the GMPE provides a normal distribution of log(Sa) with a constant standard deviation with respect to M. It can be observed that by increasing IM_0 the exceedance probability decreases more rapidly for Z_2 with respect to Z_1 which explains the trend of Figure20a. These conclusions are confirmed by disaggregation results for Tr = 50 and 2475yr reported in Figure 21a and Figure 21b where it is shown that the site can be

considered as bimodal for Tr = 50yr and unimodal for Tr = 2475yr.

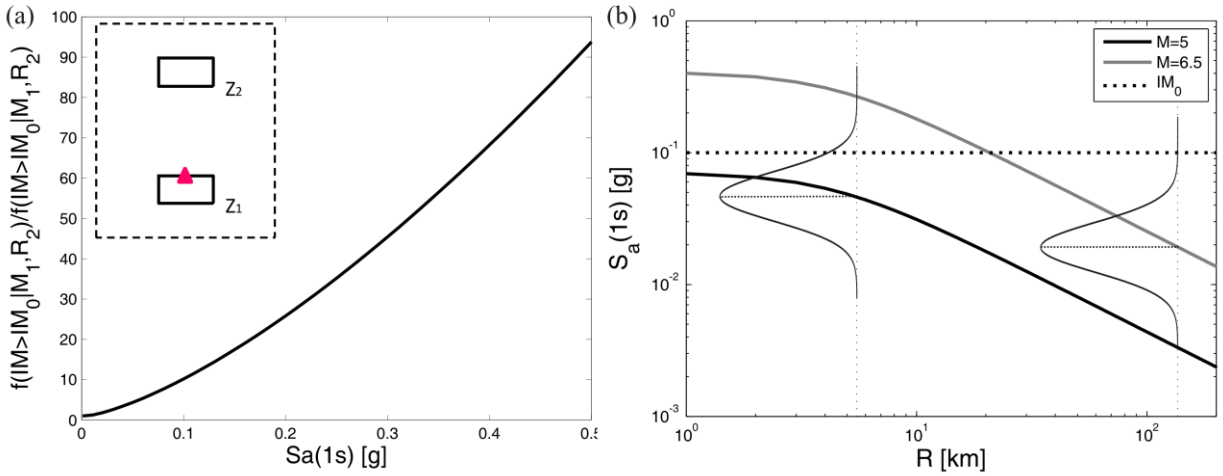

Figure 20. Sa(T = 1.0s) predicted by Ambraseys et al. GMPE for fixed magnitude values (a) and ratio of CCDFs referred to Z1 and Z2.

These conclusions[9] are confirmed by disaggregation results for Tr = 50 and 2475yr reported in Figure 21a and 21b where it is shown that the site can be considered as bimodal for Tr = 50 and unimodal for Tr = 2475yr. For the example in the figures it is assumed characteristic magnitude for the two zones and epicenters uniformly distributed within these.

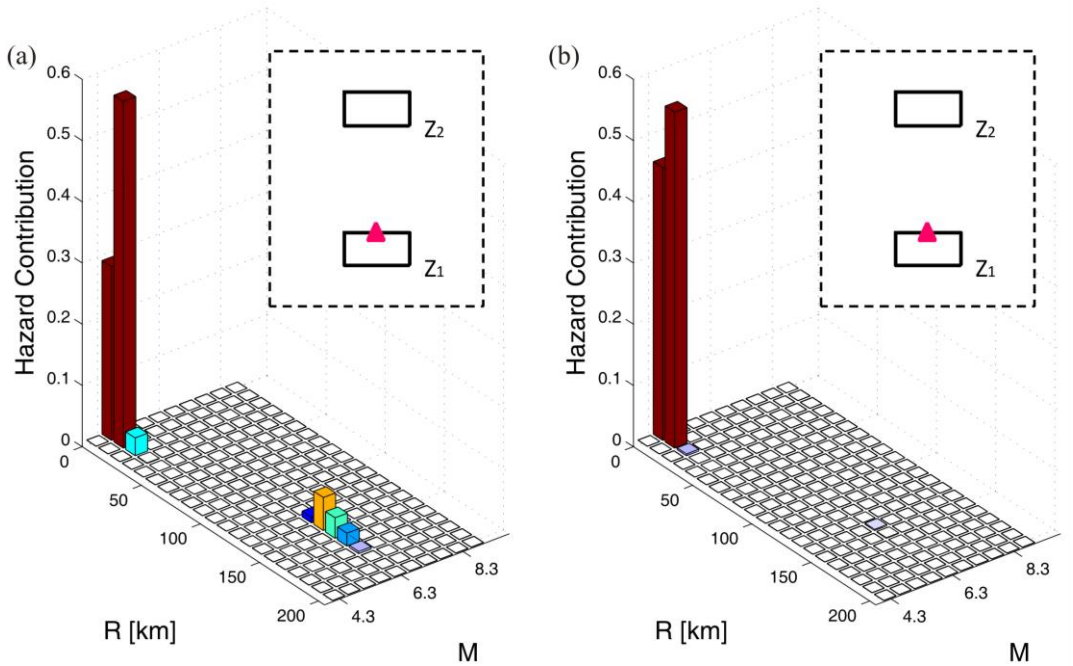

Figure 21. Disaggregation results for Sa(1s) referring to Tr = 50yr (a) and 2475yr (b).

[9] It is important to underline that earthquake occurrence rates of the zones have influence on the determination of the hazard values. If the zone with higher average Sa(1s) (Z_1 in this case) has also an higher υ rate, the influence of the second zone is practically negligible also for low Tr (so disaggregation results don't change significantly with Tr). For presentation purposes, in the example υ rate associated to Z_1 is lower than that associated to Z_2 (0.08 and0.65 respectively).

Finally, it is to note that an alternate case can occur when magnitudes and distances associated to the closer zone produce average IMs lower than that due to the more distant zone. In fact, the hazard contribution that becomes negligible for higher Tr is that of the closer zone and the second scenario results of increasing importance. Frosinone (13.336° E, 41.639° N) is one of these cases as depicted in Figure 22a and Figure22b.

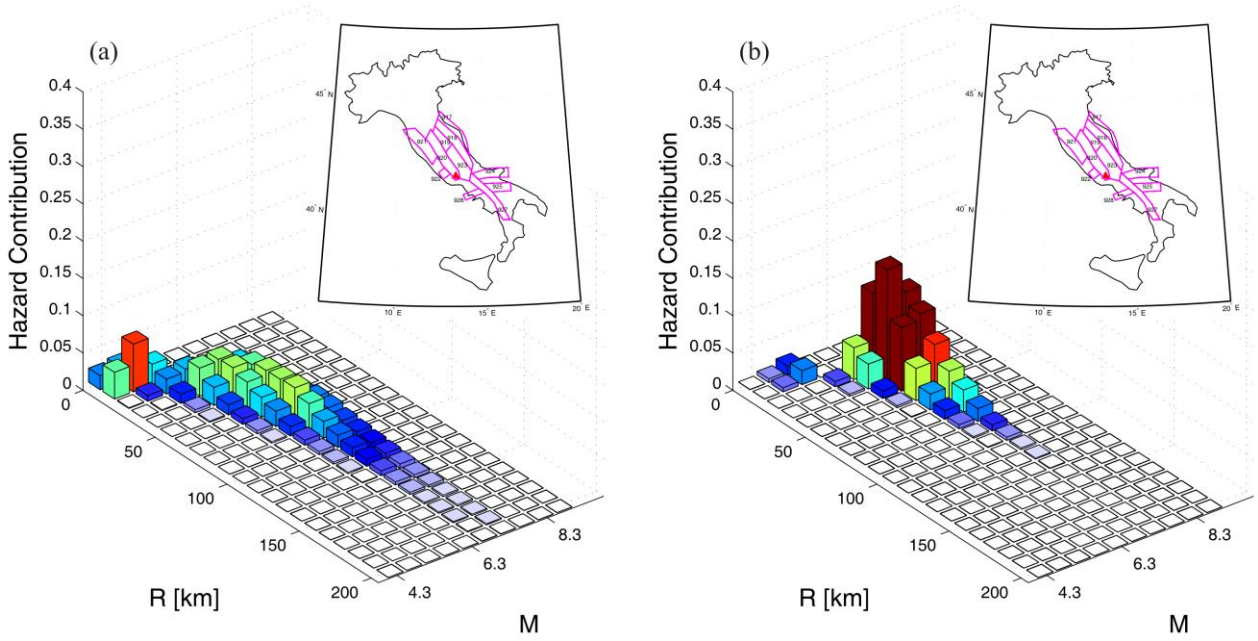

Figure 22. Disaggregation results for Frosinone at Sa(1s) for Tr = 50yr (a) and 2475yr (b).

5. Practice-ready engineering applications

5.1 Ground motion record selection for seismic structural analysis

Design may aid ground motion record selection for dynamic analysis of structures. Indeed, results of the study herein presented were included in the latest release of REXEL, a freeware software available at http://www.reluis.it/index.php?lang=en, which searches for suites of waveforms, currently from the European Strong motion Database and the ITalian ACcelerometric Archive, compatible on average to various types of code-based or user defined spectra [20]. In fact, the suites of records REXEL searches for are compatible to the reference (i.e., target) spectra complying with European code provisions, but selection criteria also reflect some research findings relevant for seismic structural assessment. In particular, REXEL 3.1 (beta) enables the selection of spectrum-

matching records corresponding to a given range of, PGA, peak ground velocity (PGV), *Cosenza and Manfredi index* (I_D) [21], *Arias Intensity*, and most importantly, M and R.

Because of implementation of these results in REXEL, choosing an Italian site and a return period (function of destination of the considered structure according to the Italian code), the software provides tridimensional disaggregation PDFs related to PGA or Sa(1s) hazard at the closest of the four return periods computed herein. Suggesting to the user the DEs to be considered as preliminary criterion for record selection, it is possible to force REXEL to search for spectrum-matching records within the M and R bins most contributing (i.e., consistent) to the hazard the target spectrum refers to (Figure 23).

5.2 Conditional hazard

Another possible use of design earthquakes is simplified vector-valued seismic hazard analysis [22]. Vectors of IM are currently under investigation by earthquake engineering research as they can improve estimation of structural response. An example of vector-valued IM may be PGA and I_D, which is the ratio of the integral of the acceleration squared to the PGA and peak ground velocity, PGV, Eq. (5). I_D is a measure related with the cyclic content of ground motion. In fact, acceleration-based IMs (e.g., PGA or spectral ordinates) have been shown to be important in the assessment of displacement structural response of buildings, but there are cases in which the cumulative damage potential of the earthquake is also of concern and therefore parameters as I_D may be relevant, although with a secondary role with respect to acceleration.

$$I_D = \frac{1}{PGA \cdot PGV} \int_0^{t_E} a^2(t)\,dt \tag{5}$$

While computing hazard analysis for vectors of IM is demanding, an easy yet hazard-consistent way of including secondary IMs in record selection is represented by the *conditional hazard maps* [23]; i.e., maps of secondary ground motion intensity measures conditional, in a probabilistic sense, to the design hazard for the primary parameter for which an hazard map is often already available by national authorities.

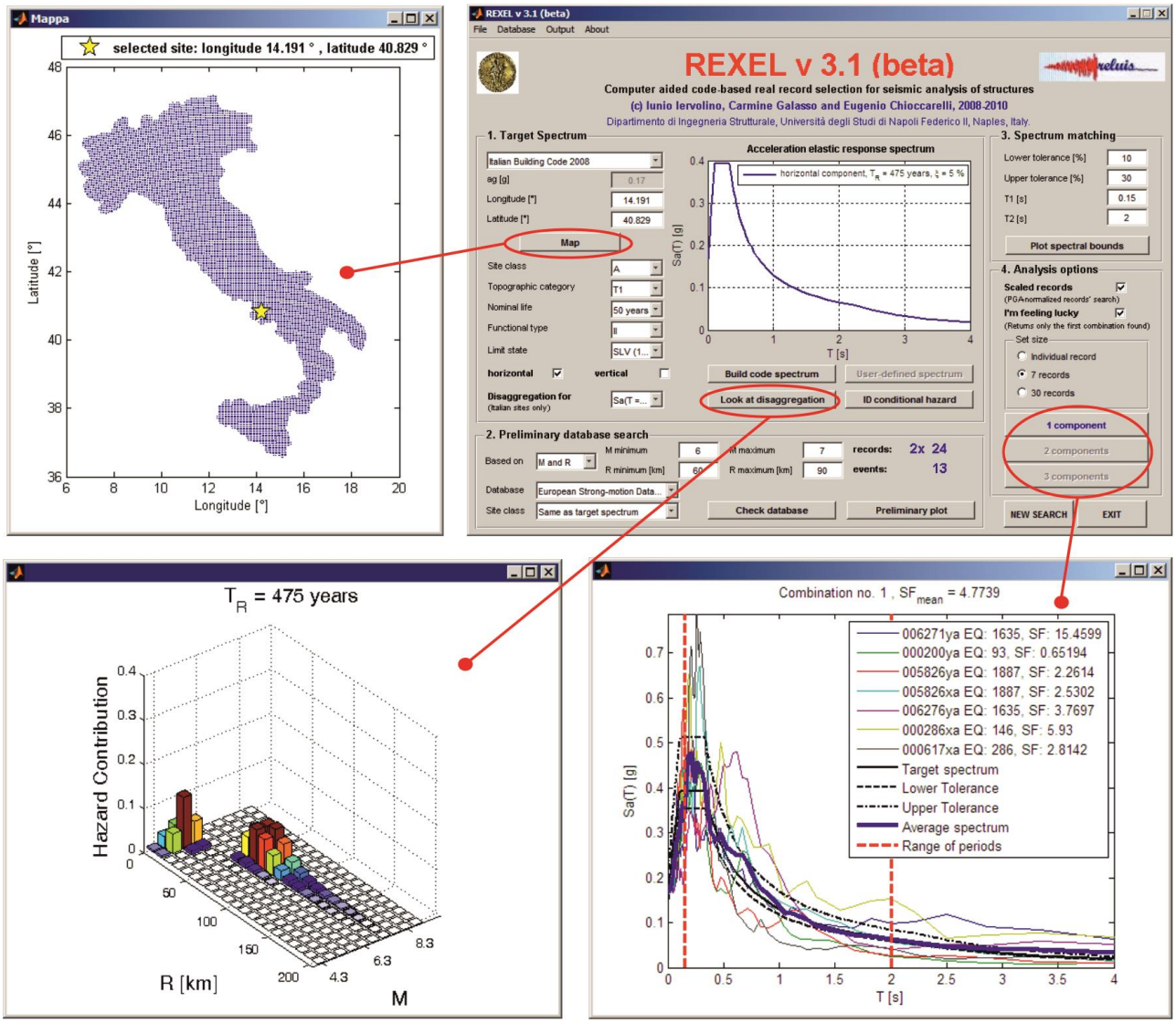

Figure 23. REXEL software, from upper left corner clockwise: selected site, software user interface and target design spectrum for life-safety limit state according to Italian code, disaggregation for Sa(1s) in terms of M and R, selected suite of records reflecting design earthquakes and matching the target spectrum.

Conditional hazard consists of computing probabilistic distribution for the secondary IM conditional to the design value of the primary IM. This requires a measure of correlation of the two IMs (e.g., [24]), and design earthquakes from disaggregation of hazard for the primary IM, to be available. In fact, it is possible to prove that under some hypotheses, the distribution of the logs of I_D conditional to the log of PGA $\left(\log_{10}\text{PGA} = z\right)$ is Gaussian with mean $\left(\mu_{\log_{10}I_D|\log_{10}\text{PGA}}\right)$ and standard deviation $\left(\sigma_{\log_{10}I_D|\log_{10}\text{PGA}}\right)$ which may be approximated by Eq. (6). Mean and standard deviation are a function of: (i) the average and standard deviation $\left(\mu_{\log_{10}I_D};\sigma_{\log_{10}I_D}\right)$ from the GMPE

for I_D; (ii) the correlation coefficient between the logs of PGA and I_D (ρ); and (iii) the average and standard deviation $\left(\mu_{\log_{10}\text{PGA}|M,R};\sigma_{\log_{10}\text{PGA}}\right)$ from the PGA GMPE. Because the conditional distribution of the logs of I_D to the logs of PGA depends on the I_D attenuation and from the PGA attenuation, it also depends on magnitude and distance; e.g., the design earthquakes {M*,R*}.

$$\mu_{\log_{10}I_D|\log_{10}\text{PGA}} \approx \mu_{\log_{10}I_D|M^*,R^*} + \rho\cdot\sigma_{\log_{10}I_D}\frac{z-\mu_{\log_{10}\text{PGA}|M^*,R^*}}{\sigma_{\log_{10}\text{PGA}}};\quad \sigma_{\log_{10}I_D|\log_{10}\text{PGA}} = \sigma_{\log_{10}I_D}\sqrt{1-\rho^2} \qquad (6)$$

With this very simple relationships and using first modal DEs discussed in this work, conditional hazard maps of I_D can be easily produced for all the Italian sites. An example is reported in Figure 24 where two percentiles of the I_D PDF conditional to PGA with a Tr = 475yr are shown.

Conditional hazard (which may be virtually extended to any pair of IMs) is also implemented in REXEL and may be used as an additional criterion for record selection in REXEL.

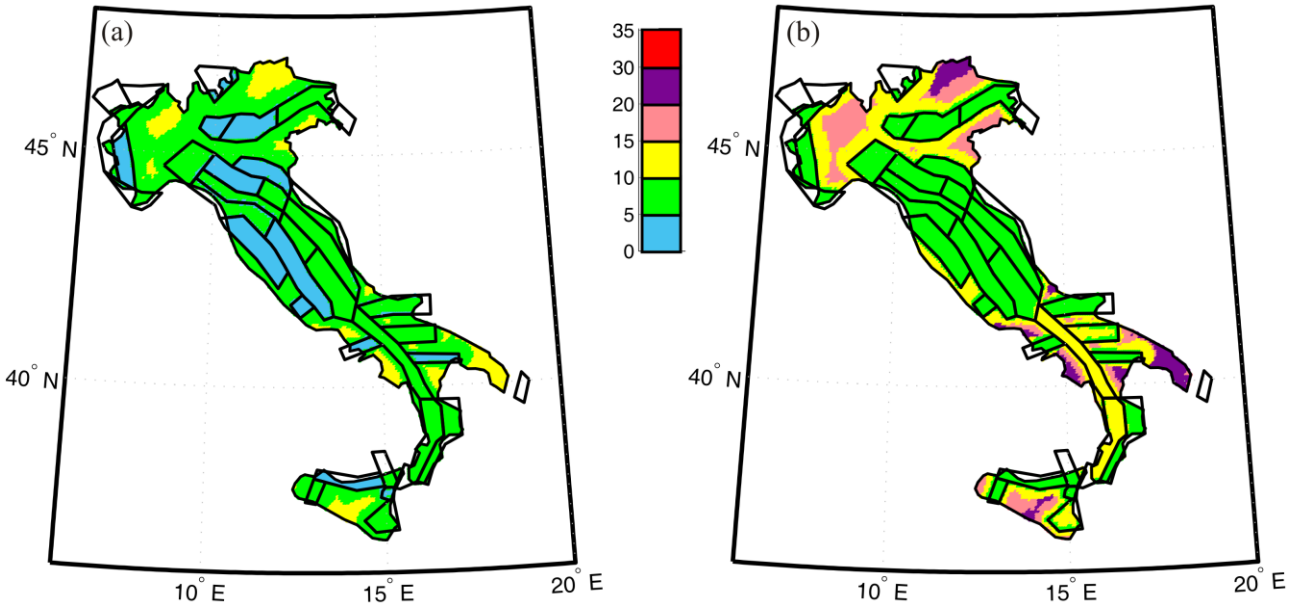

Figure 24. Maps of I_D in terms of 50th (a) and 90th (b) percentiles conditional to PGA with a 475yr return period and using first DEs of Figure 6.

Conclusions

Referring to geometric modeling of seismic source zones adopted to produce Italian hazard data to which the building code is based on, and to activity parameters from literature, design scenarios

were investigated in this study focusing on practical engineering use. Two different spectral periods equal to 0s (PGA) and 1.0s and four different return periods (50yr, 475yr, 975yr and 2475yr) were considered for hazard and disaggregation analyses.

Maps of first and second modal values of distance, magnitude and ε were shown as synthetic representation of design earthquakes. Moreover, extended disaggregation results for several sites were analyzed to demonstrate some general findings related to the given maps: (i) the first mode corresponds to an earthquake caused by the closer source (or the source the site is enclosed into) and with low-to-moderate magnitude, (ii) the second mode accounts for the influence of the more distant zones usually with larger magnitude, and (iii) moving from PGA to Sa(1s), the number of sites with at least two design earthquakes increases.

It was shown that sites enclosed or close to a seismic source zone with comparatively high seismicity (with respect to other zones affecting the hazard at the site) are characterized by an unimodal disaggregation PDF and, therefore, a single design earthquake can be identified. In the most of Italian cases two design scenarios show up, and in particular conditions, three design earthquakes give non-negligible hazard contribution. Dependency of disaggregation form spectral and return periods was demonstrated and some ideal examples were shown.

Finally a discussion on possible practical applications of the results of this study was provided. First, it was describe how disaggregation distributions for all Italian sites presented in this work have been implemented in a software, REXEL, built to search for suites of spectrum matching records. Secondly, the use of design earthquakes to build hazard curves for secondary intensity measures conditional to design value of acceleration was briefly reviewed.

Design earthquakes and consequent conditional hazard maps (also implemented in REXEL), seem easy to implement tools which can complement hazard maps to improve seismic action definitions in building codes.

Acknowledgements

The study presented in this paper was developed within the activities of "*Rete dei Laboratori Universitari di Ingegneria Sismica* – ReLUIS" for the research program funded by the "*Dipartimento della Protezione Civile"* (2010–2013). Authors want to thank Racquel K. Hagen of Stanford University who proofread the manuscript.

References

[1] Iervolino I., Maddaloni G., Cosenza E. (2008) Eurocode 8 compliant real record sets for seismic analysis of structures, *Journal of Earthquake Engineering*, 12: 54-60.

[2] Iervolino I., Maddaloni G., Cosenza E. (2009) A note on selection of time-histories for seismic analysis of bridges in Eurocode 8, *Journal of Earthquake Engineering*, 13: 1125–1152.

[3] CEN, European Committee for Standardization TC250/SC8/ (2003) *Eurocode 8: Design Provisions for Earthquake Resistance of Structures, Part 1.1: General rules, seismic actions and rules for buildings*, PrEN1998-1.

[4] McGuire, R.K. (2004) *Seismic Hazard and Risk Analysis, Earthquake Engineering Research Institute Publication*, Report MNO-10, Oakland, CA, USA.

[5] Reiter, L. (1990) *Earthquake Hazard Analysis, Issues and Insights*, Columbia University Press, NY.

[6] Baker, J.W. (2011) The Conditional Mean Spectrum: A Tool for Ground Motion Selection, *Journal of Structural Engineering*. (in press)

[7] CS.LL.PP. (2008) DM 14 gennaio 2008 Norme Tecniche per le Costruzioni, *Gazzetta Ufficiale della Repubblica Italiana*, 29. (in Italian)

[8] Bazzurro, P., Cornell, C.A. (1999) Disaggregation of Seismic Hazard, *Bulletin of Seismological Society of America*, 89: 501–520.

[9] Convertito, V., Iervolino, I., Herrero, A. (2009) Importance of Mapping Design Earthquakes: Insights for the Southern Apennines, Italy, *Bulletin of Seismological Society of America*, 99: 2979-2991.

[10] Bommer, J.J. (2004) Earthquake Actions in Seismic Codes: Can Current Approaches Meet the Needs of PBSD? in *Performance Based Seismic Design Concepts and Implementation*, PEER Rept. 2004/05, Pacific Earthquake Engineering Research Center, University of California, Berkeley, US.

[11] Meletti, C., Galadini, F., Valensise, G., Stucchi, M., Basili, R., Barba, S., Vannucci, G., Boschi, E. (2008) A Seismic Source Zone Model for the Seismic Hazard Assessment of the Italian Territory, *Tectonophysics*, 450:

85–108.

[12] Barani, S., Spallarossa, D., Bazzurro, P. (2009). Disaggregation of Probabilistic Ground Motion Hazard in Italy, *Bulletin of Seismological Society of America*, 99: 2638-2661.

[13] Barani, S., Spallarossa, D., Bazzurro, P. (2010) Erratum to Disaggregation of Probabilistic Ground-Motion Hazard in Italy, *Bulletin of the Seismological Society of America*, 100: 3335-3336.

[14] Ambraseys, N.N., Simpson, K.A., Bommer, J.J. (1996) Prediction of Horizontal Response Spectra in Europe, *Earthquake Engineering and Structural Dynamics*, 25: 371-400.

[15] Joyner, W.B., Boore, D.M. (1981). Peak Horizontal Acceleration and Velocity from Strong-Motion Records Including Records from the 1979 Imperial Valley, California, Earthquake, *Bulletin of Seismological Society of America*, 71: 2011–2038.

[16] Gruppo di Lavoro (2004) *Redazione della Mappa di Pericolosità Simica Prevista dall'Ordinanza PCM 3274 del 20 Marzo 2003*, Rapporto conclusivo per il Dipartimento della Protezione Civile, INGV, Milano-Roma, 65pp. (in Italian)

[17] Stucchi, M., Meletti, C., Montaldo, V., Crowley, H. Calvi, G.M. Boschi, E. (2011) Seismic Hazard Assessment (2003-2009) for the Italian Building Code, *Bulletin of Seismological Society of America*. (in press)

[18] Chioccarelli, E. (2010). *Design Earthquakes for PBEE in Far-Field and Near-Source Conditions*, PhD Thesis, Dipartimento di ingegneria Strutturale, Università degli Studi di Napoli Federico II, Italy. Advisors: G. Manfredi and I. Iervolino. Available at: http://www.dist.unina.it/doc/tesidott/PhD2010.Chioccarelli.pdf

[19] Iervolino I., Manfredi G. (2008) A review of ground motion record selection strategies for dynamic structural analysis. In Modern Testing Techniques of Mechanical and Structural Systems, Oreste S. Bursi, David J. Wagg (Editors), CISM Courses and Lectures 502, Springer.

[20] Iervolino, I., Galasso, C., Cosenza, E. (2010). Rexel: Computed Aided Record Selection for Code-Based Seismic Structural Analysis, *Bulletin of Earthquake Engineering*, 8: 339-362.

[21] Manfredi, G. (2001). Evaluation of Seismic Energy Demand, *Earthquake Engineering and Structural Dynamics*, 30: 485-499.

[22] Bazzurro, P., Cornell, C.A. (2002) Vector-valued Probabilistic Seismic Hazard Analysis (VPSHA), Proceedings of *7th U.S. National Conference on Earthquake Engineering*, Boston, MA, July 21-25, Paper No. 61.

[23] Iervolino, I., Giorgio, M., Galasso, C., Manfredi, G. (2010) Conditional Hazard Maps for Secondary Intensity Measures, *Bulletin of Seismological Society of America*, 100: 3312-3319.

[24] Baker, J.W., Cornell, C.A. (2006) Correlation of Response Spectral Values for Multi-Component Ground Motions, *Bulletin of the Seismological Society of America*, 96: 215-227.